

# Theory of electronic structure evolution in GaAsN and GaPN alloys

P. R. C. Kent and Alex Zunger

National Renewable Energy Laboratory, Golden, Colorado 80401

(Received 19 March 2001; published 31 August 2001)

Using the empirical pseudopotential method and large atomistically relaxed supercells, we have systematically studied the evolution of the electronic structure of  $\text{GaP}_{1-x}\text{N}_x$  and  $\text{GaAs}_{1-x}\text{N}_x$ , from the dilute nitrogen impurity regime to the nascent nitride alloy. We show how substitutional nitrogen forms perturbed host states (PHS) inside the conduction band, whereas small nitrogen aggregates form localized cluster states (CS) in the band gap. By following the evolution of these states and the “perturbed host states” with increasing nitrogen composition, we propose a new model for low-nitrogen-content  $\text{GaAs}_{1-x}\text{N}_x$  and  $\text{GaP}_{1-x}\text{N}_x$  alloys: As the nitrogen composition increases, the energy of the CS is pinned while the energy of the PHS plunges down as the nitrogen composition increases. The *impurity limit* (PHS above CS) is characterized by strongly localized wave functions, low pressure coefficients, and sharp emission lines from the CS. The *amalgamation limit* (PHS overtake the CS) is characterized by a coexistence of localized states (leading to high effective mass, exciton localization, Stokes shift in emission versus absorption) overlapping delocalized PHS (leading to asymmetrically broadened states, low temperature coefficient, delocalized  $E_+$  band at higher energies). The *alloy limit* (PHS well below CS) may not have been reached experimentally, but is predicted to be characterized by conventional extended states. Our theory shows that these alloy systems require a polymorphous description, permitting the coexistence of many different local environments, rather than an isomorphous model that focuses on few impurity-host motifs.

DOI: 10.1103/PhysRevB.64.115208

PACS number(s): 71.55.Eq, 71.70.-d

## I. INTRODUCTION: PHENOMENOLOGY OF NITROGEN-SUBSTITUTED GaP AND GaAs ALLOYS

The mixed-anion  $\text{GaAs}_{1-x}\text{N}_x$  and  $\text{GaP}_{1-x}\text{N}_x$  systems are among the classic semiconductor alloys studied in the nitrogen-dilute ( $\sim 10^{17} \text{ cm}^{-3}$ ) form since the 1960s.<sup>1,2</sup> With the advent of vapor-phase crystal growth techniques, it became recently possible to dramatically increase the nitrogen content (to  $\sim 10^{20} \text{ cm}^{-3}$ ), thus observing the evolution of this system from the impurity limit to the alloy. Interest in these systems has also increased because of the development of light-emitting<sup>3</sup> and photovoltaic<sup>4</sup> devices. These mixed-anion  $\text{GaP}_{1-x}\text{N}_x$  and  $\text{GaAs}_{1-x}\text{N}_x$  alloys distinguish themselves from the more conventional isovalent III-V alloys ( $\text{GaAs}_x\text{P}_{1-x}$ ,  $\text{GaIn}_x\text{P}_{1-x}$ ,  $\text{GaIn}_x\text{As}_{1-x}$ ), in which a first-row element is not involved. Three nitrogen regimes can be distinguished.

In the ultradilute regime (nitrogen concentration  $x < 0.01\%$ ) one observes the following.

(i) *Localized, single-impurity levels appear near the band gap.*<sup>1,2,5-7</sup> Absorption and photoluminescence excitation (PLE) of  $\text{GaP:N}$  and  $\text{GaAs:N}$  show the “ $\text{N}_x$  center” due to anion-substitutional isolated nitrogen (we use the notation  $\underline{A}\underline{B}:C$ , to denote that an isolated  $C$  atom is substituted for  $B$ , the underlined species). In  $\text{GaP:N}$  this level appears as an impurity-bound exciton at  $\bar{E}_{\text{CBM}} - 33 \text{ meV}$  below the conduction-band minimum (CBM),<sup>1,2,5,6</sup> whereas in  $\text{GaAs:N}$  it appears as a *sharp resonance* at  $E_{\text{CBM}} + 180 \text{ meV}$  (Refs. 7–10) above the CBM. In contrast, in conventional isovalent alloys such as  $\text{GaAs:P}$  or  $\text{GaAs:In}$  the ensuing perturbation potential  $V_{\text{As}} - V_{\text{P}}$  or  $V_{\text{Ga}} - V_{\text{In}}$  is too weak to create a bound state.

(ii) *Anomalously small pressure dependence of single impurity states is observed.* Shallow, effective-mass like impurity levels ( $\underline{\text{GaAs}}:\text{Zn}$  or  $\underline{\text{GaAs}}:\text{Si}$ ) are constructed from the wave function of the single nearest host crystal state. Consequently, when pressure is applied, such impurity levels change their energy at the same rate as the energetically nearest host crystal state.<sup>11</sup> In contrast, the impurity levels in dilute  $\text{GaP:N}$  and  $\text{GaAs:N}$  have anomalously small pressure coefficients: In  $\text{GaP:N}$  the energy of the impurity-bound exciton is almost pressure independent<sup>12,13</sup> ( $a_p \sim 1 \text{ meV/GPa}$ ), whereas the  $X_{1c}$  CBM of the GaP host crystal descends at a rate of  $-14 \text{ meV/GPa}$ . Thus, the impurity level in  $\text{GaP:N}$  becomes *shallower* as pressure is applied. In  $\text{GaAs:N}$ , the nitrogen level moves with pressure to higher energies at a much slower rate [ $\sim 40 \text{ meV/GPa}$  (Refs. 9 and 10)] than the  $\Gamma_{1c}$  CBM of GaAs (Ref. 14) ( $+110 \text{ meV/GPa}$ ). Thus, the impurity level becomes *deeper* as pressure is applied, emerging eventually as a discrete level into the gap at a pressure  $\sim 2.2 \text{ GPa}$ .<sup>9,10</sup> Such small pressure coefficients of electronic states are usually indicative of localization, whereby the wave function is constructed from many bands of the host crystal, rather than from the nearest host crystal state.<sup>15</sup>

In the intermediate concentration regime, one observes the following.

(iii) *Sharp photoluminescence (PL) lines appear due to impurity clusters.* Even random substitution of impurities onto the atomic sites of a host crystal creates, by chance, impurity pairs and higher-order clusters. In conventional isovalent III-V alloys, such pairs give rise to broad resonances, *within* the valence and conduction continua,<sup>16-20</sup> but no gap levels. In contrast, in GaPN and GaAsN, the N-N pairs form discrete levels inside the band gap extending in GaP down to  $E_{\text{CBM}} - 160 \text{ meV}$  (Refs. 6 and 21–23) and in GaAs down to

$E_{\text{CBM}} - 10$  (Refs. 10,9 and 24) or  $E_{\text{CBM}} - 80$  meV (Refs. 25–27). These levels and their associated phonon replica<sup>28</sup> are observed in emission after excitation into higher states. Excitation is then efficiently transferred<sup>29,30</sup> to the deeper pair levels via tunneling (at low temperatures) or via thermal excitation to the mobile states, followed by hopping into the pair levels (at higher temperatures). The pressure coefficients of these pair levels in  $\text{GaAs}_{1-x}\text{N}_x$  [35–50 meV/GPa (Ref. 10)] are as low as those of the isolated nitrogen, while in  $\text{GaP}_{1-x}\text{N}_x$  they now have *positive* pressure coefficients of  $\sim 10\text{--}30$  meV/GPa,<sup>12,13</sup> unlike the negative,  $-14$  meV/GPa value characteristic of the GaP CBM or the near zero value for the dilute impurity.<sup>13,12</sup>

(iv) *Redshift between absorption/PLE and emission is observed.* Already at a concentration of 0.05–0.1 % nitrogen in GaAs, the emission lines are redshifted with respect to absorption.<sup>31</sup> At higher concentrations the shift increases in energy,<sup>32,25</sup> in contrast with high structural quality random, direct-gap III-V alloys, where absorption and emission occur at the same energy.

As the concentration of nitrogen increases further, one observes the following.

(v) *Composition pinning of the impurity pair energy levels is seen.* The sharp emission lines from the pair levels remain initially at a fixed energy as the nitrogen composition increases both in  $\text{GaP:N}$  (Ref. 33) and in  $\text{GaAs:N}$  [0.05–0.1 % (Ref. 31)]. This surprising pinning suggests that the impurities do not interact with each other. This behavior is characteristic of deep transition-metal impurities in semiconductors,<sup>34,15</sup> but not of hydrogenic impurities (Si:P,As), which readily broaden into bands and shift in energy as their concentration increases.<sup>35</sup> In  $\text{GaAs}_{1-x}\text{N}_x$  and  $\text{GaP}_{1-x}\text{N}_x$ , as the concentration increases further, the PL from pair states acquires an asymmetric line shape with a sharp cutoff at high energy and a lingering tail at low energy.<sup>36,23,37–39</sup> The carrier decay time in these tails is anomalously long.<sup>40,30,38</sup> At yet higher concentration all of the pair/cluster lines disappear into a single, broad emission line.<sup>28,33,39</sup> This behavior contrasts sharply with conventional III-V alloys such as  $\text{In}_{1-x}\text{GaAs}_x$  where the emission line is featureless at *all alloy compositions*.

Once all of the sharp lines of pairs/clusters disappear into a single line, additional unexpected effects are seen in nitride alloys:

(vi) *The band gap shows huge, composition-dependent optical bowing.* In conventional  $A_xB_{1-x}C$  isovalent III-V alloys the band gap  $E_g(x)$  changes with respect to the composition-weighted average of the constituents as

$$\Delta E_g(x) \equiv E_g(x) - [(1-x)E_{AC} + xE_{BC}] = -bx(1-x), \quad (1)$$

where the bowing coefficient  $b$  is constant and usually  $< 1$  eV. The reasons for band-gap bowing are well understood<sup>16–20</sup> (see also Sec. IV F below). In contrast, in  $\text{GaP}_{1-x}\text{N}_x$  and  $\text{GaAs}_{1-x}\text{N}_x$  the bowing is huge and composition dependent, being largest at small  $x$ :  $\sim 26$  eV at  $x < 1\%$  eV and  $\sim 16$  eV at  $x > 1\%$ .<sup>41</sup>

(vii) *The electron mass is anomalously heavy but decreases with concentration.* In pure GaAs the electron effective mass is  $0.066m_e$ .<sup>14</sup> Small amounts ( $\sim 1\%$ ) of nitrogen increase it to  $\sim 0.4m_e$  (Ref. 42) or  $(0.12\text{--}19)m_e$  (Ref. 43), but subsequent addition of nitrogen appears to reduce the electron mass.<sup>42</sup> As the Fermi energy moves further into the conduction band, the effective mass becomes higher.<sup>44</sup> In GaP, 2.5% nitrogen creates a large mass of  $\sim 0.9m_0$ ,<sup>37</sup> compared with the X-band effective masses [ $m_{\parallel}^* \sim 0.25m_e$ ,  $m_{\perp}^* \sim 4.8m_e$  (Ref. 14)]. In sharp contrast, in conventional alloys the mass changes monotonically with composition.<sup>14</sup>

(viii) *The reduction in band gap with increased temperature slows down with nitrogen addition:* Band gaps are always reduced as temperature is increased.<sup>14</sup> However, in conventional alloys the temperature coefficient is close to the concentration-weighted average over the constituents. This reduction in PL energy with increased temperature slows down dramatically with small addition of nitrogen to GaAs (Refs. 45 and 46) and GaP (Ref. 47). Furthermore, the intensity of the PL lines of conventional alloys decreases with increasing temperature, but this decrease is accelerated by nitrogen addition, especially at low temperatures.<sup>48</sup>

(ix) *The energy of the PL lines are blueshifted as the excitation power increases,*<sup>40</sup> indicating occupation of previously empty states (so excitation must now occupy higher-energy states). This is known to occur in alloys containing localized, quantum-dot-like clusters.<sup>49</sup>

(x) *The emission decay time becomes longer with decreasing emission energy.* In other words, the states that are deeper in the gap (lower emission energies) have weaker dipole transition elements (or equivalently, less  $\Gamma$  character and more off- $\Gamma$  character).<sup>50</sup>

(xi) *New, high-energy bands appear in reflectivity at higher concentration:* Electro-reflectance measurements detect a new composition-dependent band edge, called  $E_+$ , at about 0.4–0.6 eV above the band edge, called  $E_-$ .<sup>51,8,28</sup> Whereas the lowest state  $E_-$  decreases with  $x$  (“bowing”),  $E_+$  is seen to increase with  $x$ .<sup>51</sup> Klar *et al.* do not observe  $E_+$  in  $\text{GaAs}_{1-x}\text{N}_x$  until  $x > 0.4\%$ .<sup>28</sup> Cheong *et al.*<sup>52</sup> demonstrated via resonant Raman scattering that  $E_+$  is derived from nitrogen-induced  $\Gamma$ - $L$  mixing, not from isolated nitrogen impurities. At yet higher energies, around 3 eV in  $\text{GaAs}_{1-x}\text{N}_x$ , one observes<sup>53,54,28</sup> the  $E_1$  transition, which is known to encompass a large volume of the Brillouin zone containing the  $L_{1v} \rightarrow L_{1c}$  transition. One branch of this transition is nearly composition independent according to Shan *et al.*,<sup>55</sup> but changes somewhat according to Leibiger *et al.*<sup>53</sup>

(xii) *The conduction-band  $L_{1c}$  state appears split.* Kozhevnikov *et al.*<sup>56</sup> observed that the  $L_{1c}$  band of GaAs is split into an upper branch with energy increasing with nitrogen concentration, and a lower branch with decreasing energy. They interpreted these to be  $t_2(L_{1c})$  and  $a_1(L_{1c})$ .

## II. THEORETICAL OUTLOOK ON THE BASIC PHENOMENOLOGY OF NITROGEN SUBSTITUTED GaP AND GaAs ALLOYS

The experimentally noted phenomenology surrounding nitrogen in GaP and GaAs (Sec. I) manifest a duality of

behaviors. One observes *homogeneous*, bulklike characteristics, such as band-gap bowing, resonances within the continua, rigid shift of the conduction band with temperature and pressure, the appearance of new bulklike absorption edge such as  $E_+$  and a split  $E_1$ ). On the other hand, one notes characteristics of *heterogeneous* localizations centers and alloy fluctuations, such as a distribution of various nitrogen pairs and clusters whose levels are within the forbidden gap, absorption versus emission Stokes shifts, emission blue-shift upon increased excitation power, band tails with long decay times and asymmetric line shapes. We therefore consider next what type of theoretical treatment can capture the dual nature of such alloy systems.

Theoretical approaches to the electronic structure of alloys can be divided into isomorphous and polymorphous models. In an isomorphous (“single shape”) model, one considers a single (or very few) local atomic environment that spans the entire alloy structure. For example, the virtual crystal approximation (VCA) to nitride alloys<sup>57</sup> assumes that in  $\text{GaP}_{1-x}\text{N}_x$  each Ga atom is surrounded by four identical average  $\langle \text{PN} \rangle$  “virtual atoms” and the alloy is constructed by repeating this single motif. Clearly, lattice relaxation, localization, and charge-transfer effect are excluded in this high-symmetry model. The approximations lead to a very poor description, as noted by Bellaiche *et al.*<sup>58</sup> For example, the direct-indirect crossover in  $\text{GaP}_{1-x}\text{N}_x$  occurs, according to the VCA model of Baillargeon *et al.*<sup>59</sup> at  $x=47.76\%$  in stark contrast with experiment ( $x\sim 0.43\%$ ). The coherent potential approximation (CPA) to  $A_{1-x}B_x$  alloys likewise assumes that all  $A$  atoms, irrespective of their local environment, are identical. Another isomorphous alloy model is the “band anti-crossing” (BAC) model of Shan *et al.*,<sup>51</sup> in which the alloy is constructed from a single substitutional nitrogen impurity, embedded in bulk GaP or GaAs, with a composition-dependent coupling to the CBM. This model treats only the perturbed host states (PHS), but in describing the alloy in terms of a single-impurity motif, it ignores fluctuations due to inhomogeneities. The wave function is

$$\Psi = c_1|a_1(N)\rangle + c_2|a_1(\Gamma)\rangle. \quad (2)$$

where  $|a_1(N)\rangle$  is the  $a_1$ -symmetric level of an isolated nitrogen impurity in  $T_d$  symmetry with energy  $E_N$  and  $|a_1(\Gamma)\rangle$  is the  $a_1$ -symmetric CBM of GaAs with energy  $E_{a_1(\Gamma)}$ . Clearly, only  $a_1$ -symmetric objects can be described by this representation, so impurity pairs or clusters are excluded. Moreover, since only a single bulk state is allowed to couple to nitrogen, the other bulk band states (e.g.,  $X_{1c}$ ,  $L_{1c}$ ,  $X_{3c}$  in GaAs) are assumed to be unperturbed by the impurity. The energy associated with the ansatz of Eq. (2) is

$$E_{\pm} = \frac{1}{2} [E_{a_1(\Gamma)} + E_{a_1(N)}] \pm \{ (E_{a_1(\Gamma)} - E_{a_1(N)})^2 + V^2(x) \}^{1/2}. \quad (3)$$

While treating the coupling  $V(x)$  as an adjustable parameter for each value of  $x$  permits remarkable fitting of Eq. (2) to measured bulklike quantities such as composition-, pressure-, and temperature-dependent band gaps  $E_g(x)$ ,  $E_g(p)$ , and  $E_g(T)$ , the entire phenomenology of *alloy fluctuation behavior* evident experimentally remain unexplained.

Furthermore, the dimension of *evolution* of alloy states with composition is lost as the composition dependence underlying Eq. (3) is, by construction, smooth. The generalization by Lindsay and O’Reilly<sup>60</sup> has similar properties.

While the two-level model of Shan *et al.* focuses on the perturbed host states, another picture<sup>33,39</sup> focuses instead solely on cluster states induced into the band gap by the impurities. This picture associates both the bulklike properties (e.g., large band-gap bowing) and the alloy fluctuation and localization properties (e.g., large and decaying effective mass) with cluster states that are said to interact with each other and form an impurity band.

Our foregoing analysis suggest that adequate theoretical models of nitride alloys must retain both perturbed host states *and* cluster states. This dual representation requires polymorphous alloy models.

Polymorphous (“many shapes”) alloy models focus on the central property that distinguishes disordered random alloys from ordered compounds, namely the existence of a plurality of local atomic environments.<sup>16–20</sup> In  $\text{GaP}_{1-x}\text{N}_x$  for example, the Ga atom can be surrounded by five distinct near-neighbor structures,  $P_mN_{4-m}$  with  $0 \leq m \leq 4$ ; nitrogen pairs can have arbitrary separation in the alloy, etc. Even a random distribution of impurities creates by chance, such clusters. Once different local environments are acknowledged, the phenomena of localization and fluctuations follow naturally, for some impurity clusters may induce a large enough perturbation with respect to the bulk to split a level into the gap. Different cluster types then create different levels, leading to an inhomogeneous distribution. Like in the isomorphous alloy models, PHS are allowed. However, unlike such models, cluster states (CS) are also included, and these two types of states can interact.

The most natural way to study polymorphous alloys is the supercell approach. In this method one selects a supercell containing  $M$  host crystal atoms and distributes  $I$  impurity atoms ( $x=2I/M$  for ternary alloys) within this box either randomly or via some ordering ansatz. For concentrated alloys, the “best” supercell distributes the impurities so as to mimic the pair correlation functions of a perfectly random, infinite supercell (“special quasirandom structures”<sup>61</sup>). For computational convenience, periodic boundary conditions are imposed to find the electronic states of this system. The accuracy of the results increases with the supercell size,  $M$ , as the spurious cell-to-cell interaction between impurities diminishes with size. This method was applied to study isolated substitutional nitrogen impurities<sup>62</sup> ( $I=1$ ,  $M \gg 1$ ) as well as concentrated alloys ( $I \gg 1$ ).<sup>63,64,58,65</sup> Our previous studies on nitrides<sup>63,64,58,65</sup> have used an  $M=512$  atom supercell for  $0 \leq x \leq 1$  and “for each composition we distribute the mixed elements at random on the fcc anion sites,”<sup>63,58</sup> thus naturally creating a distribution of single impurities, various pairs and clusters. Unfortunately, the existence of such heterogeneous clusters in our previous calculations<sup>63,58</sup> was missed by some readers who thought that, in our work, “ordered structures were used,<sup>63,58</sup> in which pairing or clustering effects were excluded”<sup>39</sup> or that the impurities were “uniformly distributed with a separation  $N^{-1/3}$ ” rather than

TABLE I. The relative anion-cation bond lengths around isolated nitrogen and nearest neighbor (NN) nitrogen pairs in GaAs and GaP, obtained in relaxed LDA and VFF calculations. Bond lengths are expressed in fractions of the ideal bulk GaN bond length. For the nearest-neighbor (110)-oriented pair, the 8 bonds are categorized in three symmetry distinct types: (a) (001) directed bonds ( $\times 4$ ), (b) (110)-directed bonds ( $\times 2$ ) sharing a common Ga atom, and (c) the remaining (110) directed bonds ( $\times 2$ ).

System	Cell Size	Method	Relative bond length		
			Bond (a)	Bond (b)	Bond (c)
GaAs:N	Isolated	LDA	1.062		
		VFF	1.045		
	NN pair	LDA	1.040	1.091	1.065
		VFF	1.047	1.070	1.060
GaP:N	Isolated	LDA	1.052		
		VFF	1.041		
	NN pair	LDA	1.049	1.085	1.067
		VFF	1.042	1.061	1.054

being random.<sup>33</sup> This was not the case. However, the cluster states in these previous works were not analyzed in detail.

In this paper we describe theoretically how the naturally occurring nitrogen pairs and clusters affects the electronic structure of  $\text{GaAs}_{1-x}\text{N}_x$  and  $\text{GaP}_{1-x}\text{N}_x$  alloys as a function of nitrogen concentration. By considering both the “perturbed host states” and nitrogen-related “cluster states,” we explain, at least qualitatively, the experimental anomalies outlined above, centering on the duality of bulklike and localization phenomena in these alloys.

We begin by describing our methods in Sec. III. In Sec. IV we present our results for the isolated nitrogen impurity, whereas in Sec. V we present our results for nitrogen pairs and clusters. We identify several of the “nitrogen pair” lines observed in photoluminescence, and also identify the “NC” (Ref. 33) triplet level recently observed in  $\text{GaP}_{1-x}\text{N}_x$ .<sup>33</sup> Interestingly, [110] chains of nitrogen atoms form particularly localized and deep “chain states.” In Sec. VI we consider the evolution of the conduction-band edge and nitrogen-related states with increasing nitrogen concentration. We find that (i) unlike the suggestions of Refs. 33,39 the nitrogen cluster states inside the band gap do not interact sufficiently so as to broaden and form a conduction state made of a superposition of such nitrogen-induced states. Instead, we find the delocalized “perturbed host states” descend into the fundamental band gap, and overtake the cluster states one by one. (ii) Once overtaken, the conduction-band edge exhibits *alloy fluctuations*, consisting at low energy of a broad amalgamation of Fano-resonance-like localized cluster states and, at higher energy, the delocalized perturbed host states. The low-energy side of the band edge is dominated by the just swept-in CS, while the higher-energy end consists of the more extended PHS. This localized-delocalized duality in the band edge leads to exciton localization in the tail states, the Stokes shift between absorption (into PHS) and emission (from CS), an anomalous pressure dependence, and strongly modified temperature dependence of the alloy. This behavior is distinct from conventional isolavent III-V alloys that lack cluster states in the gap and have much weaker interband coupling within the perturbed host states.

### III. METHOD

To study the role of nitrogen in GaP and GaAs we use a supercell approach, where one or more substitutional nitrogen atoms are placed in a large supercell. We relax all atomic positions, and solve the Schrödinger equation for this periodically repeated supercell using the plane-wave pseudopotential method with high-quality empirically corrected pseudopotentials (EPM). Our method is nearly identical to that of Bellaiche *et al.*<sup>58</sup> We use improved pseudopotentials,<sup>66,62</sup> larger supercells for better statistics, and we analyze our results in greater detail.

To study *isolated* nitrogen we place a single nitrogen in the supercell, whereas to study *interacting* nitrogens we keep the supercell size fixed and add a varying number of nitrogens to the supercell.<sup>58,64,64,65</sup> By modeling nitride alloys with *many* nitrogens in a large supercell, we allow for symmetry breaking, relaxation, and multiband coupling not included in simpler models<sup>67</sup> using a *single* nitrogen atom in a smaller supercell. In fact, accurate modeling of the very low nitrogen concentrations where impurity physics dominates ( $x_N \leq 0.1\%$ ) requires the use of large supercells (e.g., 13 824 atoms for 0.015%; see below) that are not accessible to current first-principles methods, such as density-functional theory. Indeed, we find that the strain field resulting from the large atomic relaxation (reflecting  $\sim 20\%$  size mismatch between N and As) propagates to long distances, so small supercells are inappropriate. However, for isolated impurities the cell-size does not need to correspond to the physical concentration  $x \rightarrow 0$ . All that is needed in this limit is to avoid wave function overlap. Furthermore, large supercells are needed to study large impurity clusters. The atomic positions within each supercell are relaxed, at the appropriate Vegard’s lattice constant, using the valence force-field method<sup>68</sup> and a conjugate gradient minimization of the total strain energy. The atomic positions obtained from this model, using the force-field parameters of Ref. 63 agree with bond lengths and positions obtained from our LDA calculations in 64-atom cells to within 1%. This is illustrated in Table I.

To obtain the electronic properties of each system at the relaxed positions we solve the Schrödinger equation

$$\left[ -\frac{1}{2}\nabla^2 + \sum_{\alpha,m} v_{\alpha}(\mathbf{r}-\mathbf{R}_{\alpha,m}) \right] \psi_i(\mathbf{r}) = \epsilon_i \psi_i(\mathbf{r}), \quad (4)$$

where  $\alpha$  denotes atomic species,  $m$  runs over atoms,  $v_{\alpha}$  are the screened empirical pseudopotentials, and  $\mathbf{R}_{\alpha,m}$  are the atomic positions. Because of the local-density approximation (LDA) error in the band gap and the need to accurately reproduce measured band gaps, combined with the use of large supercells, we have adopted an alternative approach to LDA, utilizing in Eq. (4) the empirical pseudopotential  $v_{\alpha}$ . We represent the wave functions,  $\psi$ , using a plane-wave basis set.

The total supercell potential  $V(\mathbf{r})$  is written as a superposition of species and strain-dependent local pseudopotentials  $v_{\alpha}$ . The pseudopotentials are fitted to reproduce the bulk band structures of the binary alloys GaN, GaAs, GaP, at equilibrium, the band-edge deformation potentials (pressure dependence), band offsets, and effective masses. The Fourier transform of the atomic pseudopotentials is represented as

$$v_{\alpha}(q, \epsilon) = \sum_{l=1}^4 [a_{l\alpha} e^{-b_{l\alpha}(q-c_{l\alpha})^2}] [1 + a_{5\alpha} \text{Tr}(\epsilon)], \quad (5)$$

for the GaN potentials ( $\alpha = \text{Ga, N}$ ), and

$$v_{\alpha}(q, \epsilon) = a_{0\alpha} \frac{(q^2 - a_{1\alpha})}{a_{2\alpha} e^{a_{3\alpha} q^2} - 1} [1 + a_{5\alpha} \text{Tr}(\epsilon)], \quad (6)$$

for the GaAs and GaP potentials ( $\alpha = \text{Ga, As, P}$ ), where the parameters  $a_{\alpha}, b_{\alpha}, c_{\alpha}$  are fitted and  $\epsilon$  is the local strain tensor at each atomic site. The analytical form of the pseudopotentials  $v_{\alpha}$  is chosen to describe as many physical quantities as possible without overfitting the potentials. The  $\epsilon$ -dependent term includes the effect of the local environment (local strain) around each atomic site. This term is crucial to reproducing the *individual* deformation potentials  $a_{\text{CBM}}$  and  $a_{\text{VBM}}$  when the system is deformed. Large, local strains are inevitable in the impurity systems considered here due to the GaP(GaAs)-GaN bond-length mismatch.

The GaAs and GaN potentials are identical to those of Ref. 62, and the GaP potential is similar to Ref. 66, but refitted to a higher plane-wave cutoff of 7.7 Ry for consistency with the GaAs and GaN potentials. The potentials for Ga depend on the coordination of N, P, or As atoms: For the Ga atoms surrounding each nitrogen impurity we use a composition-weighted average of the fitted GaN, GaP, and GaAs potentials, respectively. This compensates effectively for the lack of charge self-consistency. Distinct from other model calculations of the isolated impurity, and N-N pairs, we make no attempt to fit experimentally determined impurity levels, so the results constitute predictions. For low-nitrogen-content alloys,  $x_N < 6\%$ , our pseudopotentials accurately reproduce<sup>62</sup> the band-edge pressure coefficients and first-principles calculated bowing parameters.

Having fixed the pseudopotentials  $\{v_{\alpha}\}$  and relaxed the atomic positions  $\{\mathbf{R}_{\alpha,m}\}$  we solve the Schrödinger equation

using the linear-scaling folded spectrum method.<sup>69</sup> Using this method we selectively solve for a few eigenstates around a reference energy without solving for, or orthogonalizing to, *all* eigenstates of the Hamiltonian. By choosing the reference energy close to the conduction- and valence-band edges we resolve the states that are of primary importance to the physics of the impurity system.

To characterize the resultant wave functions,  $\psi_i$ , and their energy levels, we analyze the wave functions in terms of their spectral decomposition<sup>70</sup> and spatial localization. By projecting the wave functions onto the underlying Bloch states,  $\phi_{n,\mathbf{k}}$ , we determine the  $\Gamma$ ,  $L$ , and  $X$  components of the states. While wave functions inevitably include some contribution from low-symmetry points, the projection onto  $\Gamma$ ,  $L$ , and  $X$  nevertheless allows us to elucidate the leading electronic couplings between impurities and host states. The localization of each state is monitored by calculating the radius from each nitrogen site at which 20% of the amplitude of eigenstate  $\psi_i$  is enclosed. This criterion allows us to distinguish between “localized” and “quasilocalized” states by comparing with data for the isolated impurity level and for a uniformly distributed charge.

Our method is different from Lindsay and O’Reilly,<sup>60</sup> who applied effective-mass methodology to this system exhibiting manifest nonhydrogenic behavior. Our method differs from the atomistically unrelaxed, perturbative pseudopotential approach of Jaros and co-workers<sup>71,72</sup> in that (i) we find it very important to relax atomic positions in view of the large differences in atomic sizes between nitrogen and the anion it replaces, and (ii) our pseudopotential has significant differences with respect to that of Jaros and co-workers: e.g., it is environment-dependent, properly accounts for the band offsets, and incorporates explicit strain dependence, all effects missing from traditional empirical pseudopotentials.

#### IV. RESULTS: THE ISOLATED NITROGEN IMPURITY IN GaAs AND GaP

##### A. Qualitative physics of isolated substitutional nitrogen in GaP and GaAs

A substitutional impurity removes the translational symmetry of the host crystal but if it is isovalent it does not change the site symmetry (i.e., no Jahn-Teller distortion). An impurity on the  $T_d$  symmetry site of the zinc-blende lattice thus breaks the translationally-mandated degeneracy of the various band-structure valleys.<sup>73</sup> The fourfold-degenerate  $L_{1c}$  valleys break into the  $a_1(L_{1c}) + t_2(L_{1c})$  states, the sixfold-degenerate  $X_{1c}$  valley<sup>74–76</sup> ( $s$ -like on anion,  $p$ -like on cation, if the origin is an anion site) breaks into the  $a_1(X_{1c}) + e(X_{1c})$  states, the  $X_{3c}$  state<sup>74–76</sup> ( $p$ -like on anion,  $s$ -like on cation, if the origin is an anion site) gives a  $t_2(X_{3c})$  representation, whereas the singly degenerate  $\Gamma_{1c}$  valley remains as  $a_1(\Gamma_{1c})$ . Higher-energy host crystal bands are also perturbed, producing, among others,  $a_1$  states of their own. For example, in the dilute nitrogen regime, an additional nitrogen localized state forms below the conduction-band minimum in GaP and above the CBM of GaAs. These states,

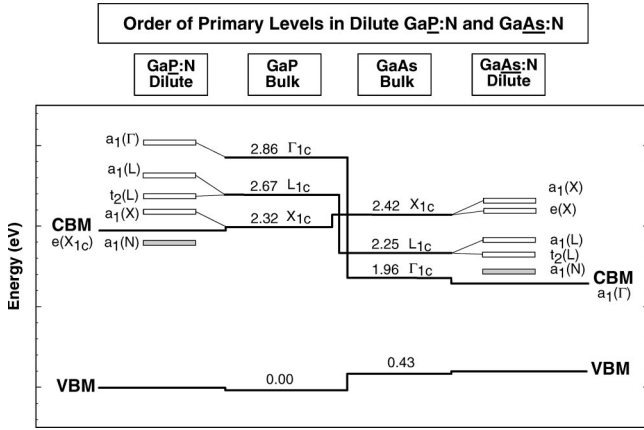


FIG. 1. Schematic of the primary bulk and impurity level order of isolated substitutional nitrogen impurities in GaP and GaAs. The GaP/GaAs band offset is 0.43 eV, taken from Ref. 77; the bulk band energies are experimental values taken from Ref. 14.

formed from many high-energy host bands, are denoted here  $a_1(N)$ . Figure 1 depicts schematically the  $a_1$ -symmetric nitrogen-perturbed states.

All states of the same symmetry representation interact under the impurity perturbation potential,  $\Delta V_{tot}$ , which consists of the following. (i) The difference in host-impurity screened potential  $\Delta V_{chem}$ : A good qualitative measure of  $\Delta V_{chem}$  is the “natural” band offset,<sup>77</sup> for example, the CBM of GaN lies  $\sim 0.3$  eV below that of GaAs and  $\sim 0.6$  eV below GaP. (ii) The perturbation due to atomic displacement  $\Delta V_{rel}$ : This second perturbation is expected to be substantial due to the lattice-constant mismatch between GaN and GaP (GaAs). The total perturbation  $\Delta V_{tot}$  mixes all  $a_1$  states (thus, mixes  $\Gamma_{1c} + X_{1c} + L_{1c}$ , etc.), separately mixes all  $t_2$  states ( $X_{3c} + L_{1c}$ ), etc. The mixing is decided by this perturbation, as well as by the proximity of the states  $\Gamma_{1c}, X_{1c}, L_{1c}$ , in the host crystal. The different ordering of these host states is depicted in Fig. 1 (using the LDA-calculated band offsets<sup>77</sup> between GaP and GaAs). Note that in GaAs the conduction level ordering is  $\Gamma_{1c} \rightarrow L_{1c} \rightarrow X_{1c}$  for  $a_1$  states, while in GaP it is  $X_{1c} \rightarrow L_{1c} \rightarrow \Gamma_{1c}$ .

## B. Quantitative results for isolated nitrogen

### 1. GaAs:N

The  $a_1$ -symmetric electron energy levels obtained by our calculation for GaAs:N are shown in Fig. 2(a) for various sizes of the GaAs supercell, ranging from 64 atoms to 13 824 atoms, each containing a single nitrogen impurity. Note that since each cell contains a single nitrogen atom, all calculations depicted in Fig. 2 correspond to models of isolated nitrogen (i.e., no pairs or higher clusters), much like the calculations Mattila *et al.*<sup>62</sup> The supercell size does not reflect nitrogen composition, but rather that an increasing number of bulk states that “fold” into the Brillouin zone and can interact with the nitrogen. Figure 2(b) shows analogous results obtained recently<sup>78</sup> via LDA calculations whose nonlocal pseudopotential was scaled to reproduce the experimental bulk band gaps. (In these calculations 4096-atom systems

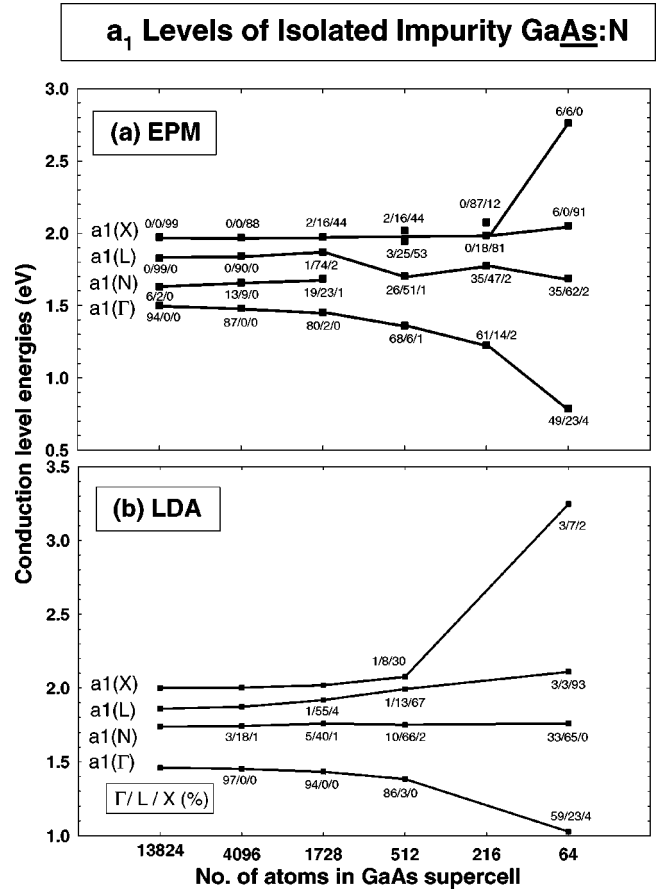


FIG. 2. Calculated energies of the  $a_1$  levels of isolated nitrogen impurities in GaAs versus supercell size using (a) EPM calculations, and (b) scaled-LDA calculations (Ref. 78) where the non-local pseudopotentials are adjusted to reproduce experimental band gaps. We also give the percentage  $\Gamma, L, X$  character of each level computed using the spectral decomposition of Ref. 70.

were made accessible to LDA by embedding the self-consistent potential of a 64-atom GaAs:N calculation within the potential of a 4096-atom bulk GaAs cell, and solving for near-gap eigenvalues.) We give for each level the percentage  $\Gamma, L$ , and  $X$  character. We see that the EPM and scaled-LDA results for GaAs:N are remarkably similar. Our  $a_1(N)$  level is at  $E_c + 150$  meV and  $E_c + 180$  meV for 4096- and 13 824-atom cells, respectively. A recent empirical calculation (where the energy of the deepest nitrogen-nitrogen level was fitted) obtained  $E_c + 106$  meV.<sup>79</sup> The experimental impurity level was estimated by Wolford *et al.*<sup>7</sup> at 150–180 meV above the CBM, and confirmed in more recent measurements.<sup>10,8</sup> We do not find a midgap  $a_1(N)$  level with two holes in it as recently suggested in the calculations of Orellana and Ferraz.<sup>80</sup>

Figures 3(a)–3(d) shows the calculated wave functions for the first four conduction  $a_1$  states in dilute GaAs:N and Figs. 3(e)–3(g) the first three  $a_1$  states in dilute GaP:N (4096 atoms). In GaAs:N, the three lowest  $a_1$  states exhibit a striking nitrogen localization, and long tails extending along the [110] directions far into the host lattice. The tail structure of the impurity states explains the strong nitrogen-nitrogen in-

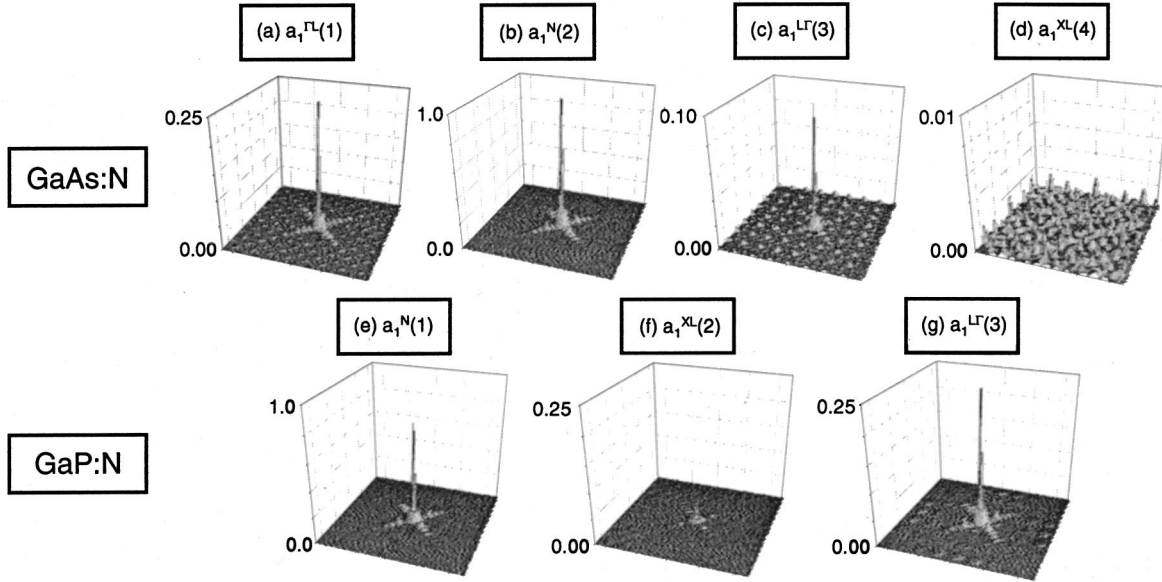


FIG. 3. The wave functions squared of the lowest energy  $a_1$  conduction states of (a)  $\text{GaAs:N}$ , and (b)  $\text{GaP:N}$  (supercell size: 4096 atoms). The  $x$ ,  $y$ ,  $z$  axes lie on the  $[100]$ ,  $[010]$ , and  $[001]$  directions, respectively.

teractions within clusters, observed particularly for  $[110]$  clusters in  $\text{GaAs:N}$ ,<sup>10</sup> which will be discussed in Sec. V C. Figures 3(b) and 3(e), the “ $a_1(N)$ ” nitrogen impurity state in  $\text{GaAs:N}$  (resonant state), and  $\text{GaP:N}$  (gap state) are remarkably similar. The  $\text{GaAs:N}$  resonant state manifests a weaker nitrogen localization than in  $\text{In GaP:N}$ .

Figure 3 also highlights the nonhydrogenic nature of nitrogen states in GaAs or GaP. For hydrogenic impurities, the wave function Bohr radius,  $r_0$ , is given by the energetic distance  $\Delta E$  to the nearest host crystal band whose effective mass is  $m^*$ , as

$$\frac{1}{r_0} = \sqrt{\frac{2m^*\Delta E}{\hbar^2}}. \quad (7)$$

Using a typical  $\Delta E$  of 7 meV,<sup>24</sup> one computes<sup>39</sup> a radius  $r_0 = 63 \text{ \AA}$ . However, our non-effective-mass calculation (Fig. 3) shows that the radius of the nitrogen state is much smaller, having a full width at half maximum of only  $\sim 6 \text{ \AA}$ . Band gap reduction is already observed in 0.1%  $\text{GaAs}_{1-x}\text{N}_x$ ,<sup>8,25,81</sup> which requires radii of order 100  $\text{\AA}$  if band-gap reduction is to occur through overlap of nitrogen impurity wave functions. Clearly, impurity wave function overlap is not the principal mechanism of bowing, in contrast with suggestion of Refs. 33 and 39. One might wonder if our prediction of strong, superhydrogenic localization of  $a_1$  states could reflect an exaggerated binding energy in our calculation. However, our calculated binding energies of  $a_1(N)$  are in accord with experiment<sup>7</sup> both for  $\text{GaAs}_{1-x}\text{N}_x$  and  $\text{GaP}_{1-x}\text{N}_x$ , as discussed above.

We now characterize these pseudopotential calculated states. The lowest  $a_1$  state, denoted  $a_1^{\Gamma L}(1)$ , whose wave function, depicted in Fig. 3(a), is the alloy’s conduction-band minimum, exhibits spatial localization and, in small supercells, strong  $\Gamma L$  mixing. The third  $a_1$  state, denoted  $a_1^{\Gamma L}(3)$ ,

whose wave function is depicted in Fig. 3(c) is the counterpart of  $a_1^{\Gamma L}$ , with a reversed proportion of  $\Gamma$  and  $L$  (favoring  $L$ ). The splitting between  $a_1^{\Gamma L}(1)$  and  $a_1^{\Gamma L}(3)$  is the effective  $\Gamma$ - $L$  coupling  $2V^{\Gamma L}$  in the alloy, about 0.5 eV at 1%, in excellent agreement with 0.5 eV measured recently in ballistic electron emission microscopy (BEEM) experiments.<sup>56</sup> This strong coupling distinguishes  $\text{GaP}_{1-x}\text{N}_x$  and  $\text{GaAs}_{1-x}\text{N}_x$  from conventional alloys, e.g.  $\text{GaAs}_x\text{P}_{1-x}$ . The second  $a_1$  state, denoted  $a_1^N(2)$ , whose wave function is shown in Fig. 3(b) is not associated with band-edge states ( $\Gamma, L, X$ ) but is composed of a large number of contributions from high-energy bulk bands and is highly nitrogen localized. For large supercells ( $\geq 4096$  atoms) its energy is just above  $a_1^{\Gamma L}(1)$  and its wave function [Fig. 3(b)] is highly localized. This is seen by the rapid rise of its “charge-accumulation function”  $Q_i(R) = \int_0^R |\Psi_i(R)|^2 dR$  with  $R$  (Fig. 4). For comparison we also show in Fig. 4 the rate of charge accumulation  $Q_i$  in a sphere of radius  $R$  for a uniform distribution. In smaller supercells, the energy of the state rises rapidly since its wave function becomes more extended [Fig. 4(c)]. This might explain why this state was not detected in previous small (64–216) supercell calculations.<sup>67</sup> With decreasing cell size both  $a_1^{\Gamma L}(1)$  and  $a_1^N(2)$  become delocalized due to the (unphysically large)  $a_1^{\Gamma L}(1)$ - $a_1^N(2)$  interaction. Finally, the fourth  $a_1$  state, denoted  $a_1^{XL}(4)$  whose wave function is depicted in Fig. 3(d) is derived from the  $X_{1c}$  conduction state. Results for the  $e^-$ - and  $t_2^-$ -derived impurity states in  $\text{GaAs:N}$  were discussed by Mattila *et al.*<sup>62</sup>

## 2. $\text{GaP:N}$

Figure 5 depicts the energies of the lowest three  $a_1$  states of isolated substitutional nitrogen in GaP. In analogy with GaAs, Figure 2, at large supercell size a localized impurity  $a_1^N$  state is formed close in energy to the  $X^-$ - and  $L^-$ -derived

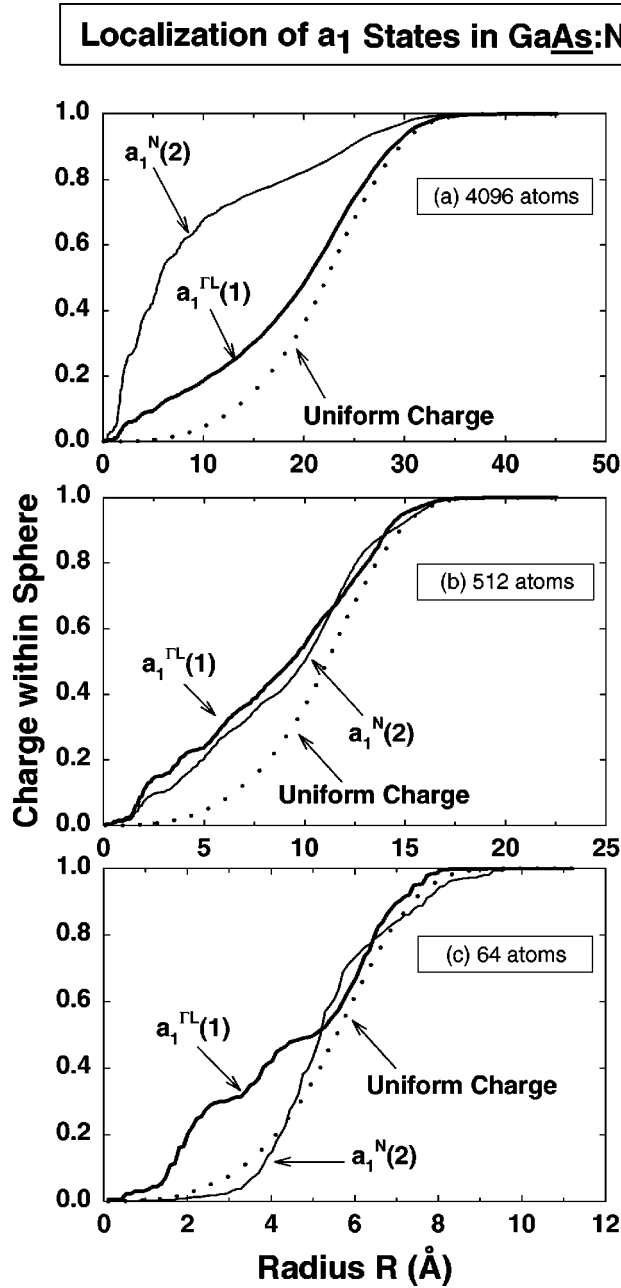


FIG. 4. The charge accumulation function  $Q_i(R) = \int_0^R |\Psi_i(R)|^2 dR$ , of the lowest energy  $a_1$  conduction states of GaAs:N as a function of the sphere radius  $R$  for several concentrations. The dotted line gives, for comparison, the charge contained within a sphere of radius  $R$  of uniform composition.

$a_1$ -symmetric states. This state appears *below* the CBM (“gap level”) whereas in GaAs the impurity level is *above* the CBM (“resonant level”). Transitions to the lowest conduction state in both materials, whether delocalized or impuritylike, are dipole allowed from the valence-band maximum (VBM) (“direct gap”). In smaller GaP supercells ( $\leq 512$  atoms) another band, with more  $L_{1c}$  character plunges down and becomes the conduction-band minimum. This state descends rapidly in energy with decreasing cell size, crossing the  $a_1^{XL}$ -derived state and becoming nitrogen localized in the

smaller cells. Figure 5 thus demonstrates the danger in representing isolated nitrogen in GaP by a cell with less than  $\sim 2000$  atoms.

Experimentally, photoluminescence measures<sup>5,6</sup> the ground state of impurity-bound excitons. We have calculated the *electron* energy level of neutral, substitutional N, which differs from the experimentally determined energy by the exciton binding energy. Our calculated electron level in GaP:N is  $\sim 30$  meV below the CBM at  $x_N = 0.01\%$ . Excitonic effects are expected to *lower* this level, rendering our level a little deeper than the experimental values of  $\sim 36$  meV.<sup>5,6,13</sup>

### C. Pressure dependence of levels of the isolated nitrogen impurity

Figures 6(a) and 6(b) shows selected calculated energy levels of GaP:N and GaAs:N as a function of pressure for the isolated impurity limit (cell size 4096 atoms). We also show the  $\Gamma$ ,  $L$ , and  $X$  character of each state.

For isolated nitrogen in GaP [Fig. 6(a)], we find an anti-crossing behavior of the lowest-energy  $a_1$ -symmetric state: The  $a_1(N)$  state is strongly repulsed by the  $a_1(X_{1c})$ , state which is close in energy (30 meV) and shares significant  $X$  character. This repulsion yields a very weak (2 meV/GPa at zero pressure) dependence, compared to the similarly weak experimental value of  $\sim -1$  meV/GPa (Ref. 13) at  $\sim 10^{18}$  impurities/cm<sup>-3</sup>, or with the pressure coefficient of  $-14$  meV/GPa of the CBM of pure GaP.<sup>82</sup> Overall, the  $a_1(N)$  level moves *down* in energy as pressure increases. We will see later (Fig. 7) that this trend is reversed at higher nitrogen concentrations. Note that since the  $e(X_{1c})$  level has no matching symmetry at this energy range, it is only weakly unperturbed and can serve as an indicator for the real GaP<sub>1-x</sub>N<sub>x</sub> CBM.

For isolated nitrogen in GaAs [Fig. 6(b)] the lowest conduction level,  $a_1(\Gamma_{1c})$ , rapidly increases in energy with applied pressure. The  $a_1(\Gamma_{1c})$  and  $a_1(N)$  impurity state strongly repel and anticross [shown in Fig. 6(b) by a dashed line], thereby changing character. The calculated anticrossing behavior depends somewhat on supercell size and is 1.5–2 GPa for 4096-atom cells and 2 GPa for larger cells. At this pressure the  $a_1(N)$  level appears as a gap state, in agreement with photoluminescence measurements that observe a level emerge from the conduction continua at  $\sim 2.2$  GPa.<sup>10</sup> This anticrossing reduces significantly the pressure dependence from 110 meV/GPa in pure GaAs to approximately half of this value in dilute GaAs<sub>1-x</sub>N<sub>x</sub>.

### D. Why is the isolated nitrogen level resonant in GaAs but inside the band gap in GaP?

Thomas, Hopfield, and Frosch<sup>1</sup> and Balderschi<sup>83</sup> expected that since nitrogen atoms are more similar to phosphorus than arsenic, in terms of electronegativity and pseudopotentials, the GaP:N impurity level will be shallower than the GaAs:N impurity level. Figures 2 and 5 show that the oppo-

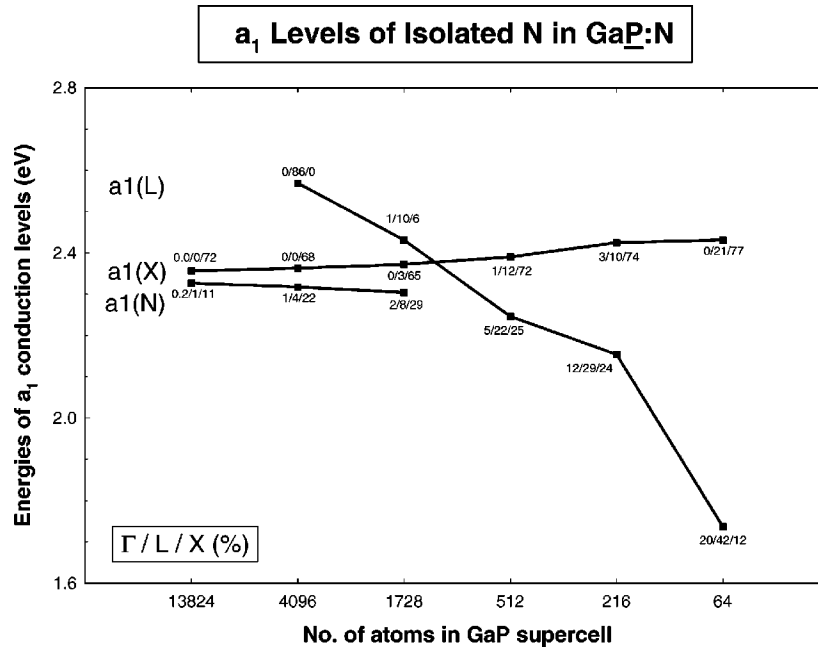


FIG. 5. Calculated energies of  $a_1$  of *isolated* nitrogen impurities in GaP versus supercell size. The percentage  $\Gamma, L, X$  character of each level is also given, computed using the spectral decomposition of Ref. 70.

site is true: the former level is  $\sim 30$  meV inside the gap, whereas the latter is  $\sim 180$  meV above the CBM. The reason is evident from Fig. 1: the band offset between GaP and GaAs (calculated in Refs. 84, 77 and 85) is such that the

CBM of GaP is higher on an absolute scale than that of GaAs by 0.43 eV, thus exposing the nitrogen level inside the GaP band gap. Indeed, until recently<sup>62,86,58,65,64</sup> the importance of correctly reproducing the band alignment in the theoretical

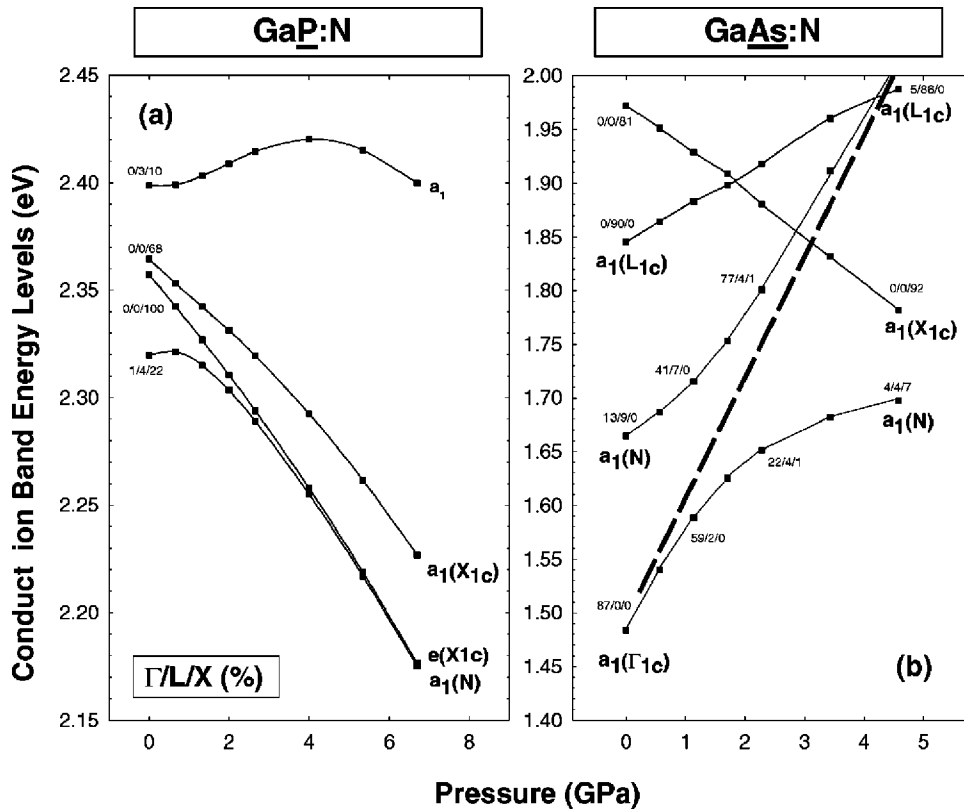


FIG. 6. The calculated pressure dependence of selected levels of isolated nitrogen for (a) GaP:N and (b) GaAs:N. We also give the percentage  $\Gamma, L, X$  character of each level as a function of pressure. As a guide to the eye, in (b) we show the pressure dependence of the bulk GaAs CBM with a dashed line (supercell size: 4096 atoms).

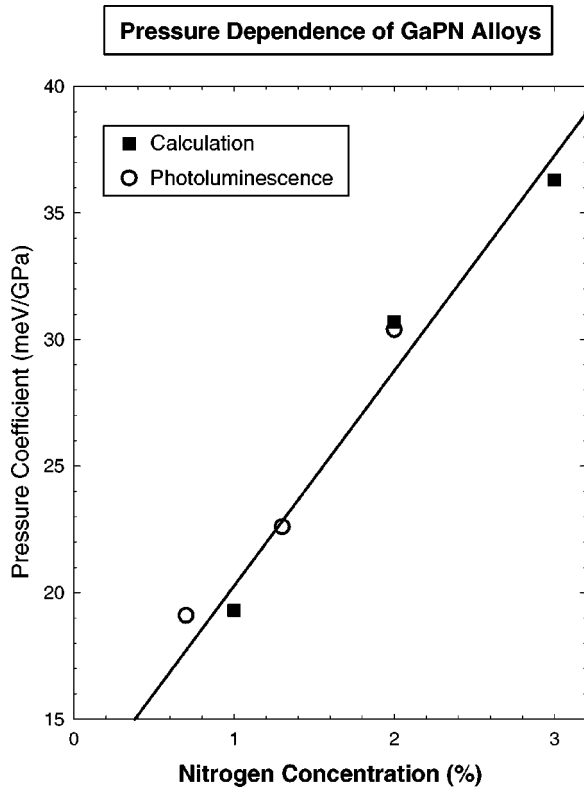


FIG. 7. Calculated pressure dependence of  $\text{GaP}_{1-x}\text{N}_x$  conduction-band minima, compared with the measurements of Ref. 54.

description of nitrogen impurities [related to the zero-momentum screened potential  $V(\mathbf{G}=0)$ ] was not recognized. Early practitioners<sup>87,71,88</sup> found pathologically deep nitrogen levels ( $\sim 1$  eV in Ref. 87), failing to properly align the “GaN” with the “GaP” potentials. A correct alignment explains the level order.

#### E. Can a two-level model capture the qualitative physics of the $a_1$ electron states for isolated nitrogen in dilute GaP:N or GaAs:N?

Hjalmarson *et al.*<sup>88</sup> noted in their tight-binding model only a single  $a_1(N)$ -type level and its corresponding  $t_2$  level (compare, however Fig. 2). Wolford *et al.*<sup>7</sup> also discussed for GaAs:N the  $a_1(N)$  and  $a_1^\Gamma$  levels. Following these works, Shan *et al.*<sup>51</sup> advanced a two-level model for the electron states of the  $\text{GaAs}_{1-x}\text{N}_x$  alloy, consisting of both of these states. By solving Eq. (3) and fitting the coupling potential  $V$  at each  $x_N$  (i.e., one adjustable parameter per data point) to various experiments, they obtained a successful phenomenological description of the data, showing anticrossing of the two levels as a function of nitrogen concentration and pressure. However, Mattila *et al.*<sup>62</sup> showed that for the composition range studied by Shan *et al.*, the  $a_1(N)$  level is no longer close in energy to  $a_1^\Gamma$  so it cannot be the origin of the observed anticrossing. Zhang *et al.*<sup>42</sup> have criticized the model of Shan *et al.* on the basis of experimental observations: resonant Raman scattering<sup>52</sup> and BEEM<sup>56</sup> experiments

demonstrate the existence of distinct  $L_{1c}$  character near the CBM, ignored by the two-level model.

The fundamental considerations of intervalley coupling<sup>73–76</sup> and their present quantitative evaluation (Figs. 2 and 3) demonstrate indeed that the basic physical picture here involves the coupling and anticrossing between *all* nitrogen-perturbed  $a_1$ -like band-edge states ( $\Gamma$ - $X$ - $L$ ), rather than the two-level model of coupling between  $\Gamma$  and a single localized  $a_1^N$ .<sup>51</sup> Our calculations show that *at least four*  $a_1$ -symmetric levels participate in the dilute nitrogen physics of  $\text{GaAs}_{1-x}\text{N}_x$ , and the nature and intervalley couplings of these states is strongly composition dependent. This is evidenced by the strong mixing of all levels (not just two of them), evidenced by the wave-function projections given, e.g., in Fig. 2. In particular, the neglect of  $L_{1c}$  mixing in the simple two-level model is noteworthy. In  $\text{GaP}_{1-x}\text{N}_x$ , our calculations show that at least three  $a_1$ -symmetric levels participate in the dilute nitrogen physics of  $\text{GaP}_{1-x}\text{N}_x$ .

The band anticrossing model has been applied to  $\text{GaAs:N}$ , where the unperturbed  $a_1(N)$  level is at 0.2 eV *above* the unperturbed host CBM. Thus, because of level repulsion the lowest state of the system is the nitrogen-modified GaAs CBM, whereas the nitrogen impurity level is higher in energy. Alloy bowing is thus measured with respect to the lowest state. For  $\text{GaP:N}$  however, the unperturbed  $a_1(N)$  lies *below* the unperturbed host CBM (see Figs. 1 and 5). The model thus predicts in  $\text{GaP}_{1-x}\text{N}_x$  that the conduction-band edge is formed directly from the nitrogen states, which cannot be the case at low concentrations (see, e.g., Ref. 33). Further comparisons with the two-level model are made in Sec. VII D.

#### F. Do isolated nitrogen impurities create anomalous bowing?

It is interesting to enquire whether the fast decrease of band gap upon nitrogen addition<sup>89,57,48</sup> is primarily due to nitrogen-host interactions, nitrogen-nitrogen interactions,<sup>42</sup> or both. To separate the effects we first have studied the band gap for isolated nitrogen as a function of supercell size. To this end we have placed a *single* nitrogen atom in a GaAs or GaP supercell, changing systematically the number of *host atoms* in the cell. The direct nitrogen-nitrogen interaction is kept small as the shortest N-N distances, 22.6 and 45.2 Å for 512 and 4096 GaAs atom cells, respectively, are kept large. As the cell size increases, more GaAs or GaP bulk states “fold in” and are available to interact with the nitrogen states, but no direct nitrogen-nitrogen interaction is allowed within a supercell as would be the case if many nitrogens were added. This construct affords direct examination of the rate of change of the band gap [Eq. (1)], isolating the effect of impurity-host interaction (present) from chemical cluster effects (absent). The latter were suggested<sup>42</sup> to be the reason for the anomalously large bowing observed in  $\text{GaAs}_{1-x}\text{N}_x$ .

Our cluster-free calculation shows that the bowing coefficient is already large for isolated nitrogen, being  $b=26$  eV for the lowest transition in  $\text{GaAs}_{1-x}\text{N}_x$ , Fig. 2, and  $b=20$  eV for  $\text{GaP}_{1-x}\text{N}_x$ , Fig. 5. Thus, nitrogen-nitrogen cluster interaction can not be the primary reason for bowing. The mechanisms leading to band gap bowing due to per-

turbed host states (in the absence of gap levels) was discussed previously in detail<sup>16–20</sup> as these are common to conventional semiconductor alloys. There are three contribution at play for random alloys.

(i) *Volume deformation*, which represents changes in the band gaps of the *constituents* GaAs and GaN that are compressed and dilated, respectively, from their natural lattice constants to the intermediate alloy value  $a(x)$ . This deformation raises the band gap of GaAs and reduces the band gap of GaN.

(ii) *Charge exchange*, which represents the change in the band gap upon bringing together the constituents, already prepared at  $a(x)$ , without yet permitting any sublattice relaxation. This term includes charge-transfer effects that result from band mixing in an ideal, unrelaxed lattice. This term is particularly large in mixed-anion nitride alloys.

(iii) *Structural relaxation* represents the change in band gap due to sublattice relaxation at fixed  $a(x)$ . This term includes atomic-relaxation-induced band mixing. In mixed-anion alloys such as  $\text{GaP}_{1-x}\text{N}_x$ , the major relaxation occurs in the *cation* sublattice; this couples primarily the cation-localized conduction states, causing the lowest to move to yet lower energies (bowing). In mixed-cation alloys, such as  $\text{InGaN}$ , the major relaxation occurs in the *anion* sublattice, which couples primarily the anion-localized valence bands, causing the highest to move to yet higher energies. Structural relaxation thus contributes to bowing in all alloys having common atoms; the effect is proportional to the size mismatch between the dissimilar atoms. The effect is particularly strongly due to large cation displacement<sup>58</sup> in  $\text{GaP}_{1-x}\text{N}_x$  and  $\text{GaAs}_{1-x}\text{N}_x$ . We conclude that mixed-anion nitride alloys have a large bowing even in the absence of cluster states because of relaxation-mediated band coupling, not nitrogen-nitrogen wave-function overlap.<sup>39</sup>

To see the dependence of bowing on concentration, we note that according to Eq. (1) (that applies only to conventional alloys) at the  $x \ll 1$  dilute limit, the band-gap change  $\Delta E_g(x)$  scales as  $-bx$ , i.e., linearly with nitrogen concentration. Fitting our calculated  $\Delta E_g(x)$  for the case that has no clusters (one nitrogen per supercell) to  $\Delta E_g \propto x^\alpha$  for  $\text{GaAs}_{1-x}\text{N}_x$  gives  $\alpha = 0.76$  using our EPM calculations and  $\alpha = 0.76$  for the LDA data of Ref. 78. We see that bowing in cluster-free  $\text{GaAs}_{1-x}\text{N}_x$  is already *anomalous* ( $\alpha < 1$ ), and pairs or other clusters are not needed to produce  $\alpha \ll 1$  in contrast with recent suggestions.<sup>90</sup> This result is due to the additional coupling between the  $a_1^{\Gamma L}(1)$  CBM and the  $a_1^N(2)$  impurity state present in  $\text{GaAs}_{1-x}\text{N}_x$  but not in normal alloys, e.g.,  $\text{GaAs}_x\text{P}_{1-x}$ . In fact, when cluster states are available in the band gap below the PHS, we find *slower bowing* with  $\alpha = 0.66$  (Sec. VII B), rather than  $\alpha = 0.76$ ; thus clusters *reduce* bowing.

### G. Does atomic relaxation make the isolated impurity level shallower?

Early calculations<sup>87</sup> of substitutional N in GaP first produced very deep gap levels,  $\sim 1$  eV from the CBM. Phillips argued<sup>91</sup> that this overestimation of the binding energy is due to the neglect of atomic relaxation that will render the level

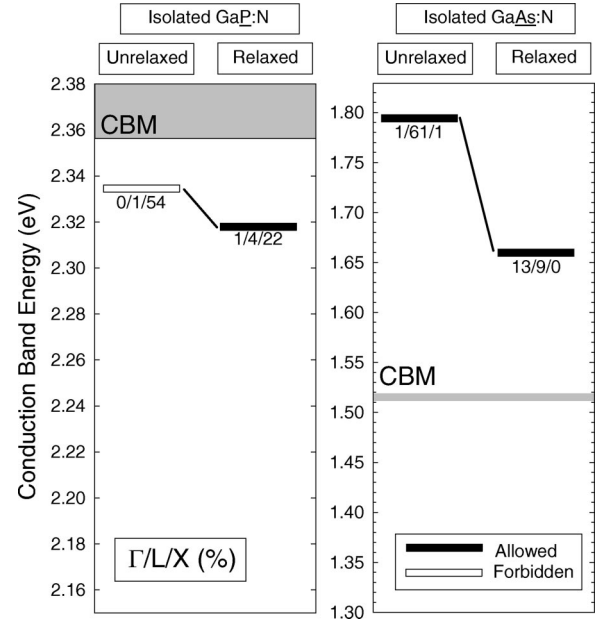


FIG. 8. The calculated energy levels of isolated nitrogen in GaAs and GaP, before and after lattice relaxation. We also denote whether a transition is allowed (finite  $\Gamma$  character) or forbidden (zero  $\Gamma$  character).

*shallower*. Jaros and Brand<sup>71</sup> indeed noted that moving the neighboring Ga atoms towards N by 0.1 a.u. *weakens* considerably the impurity potential, suggesting indeed that relaxation drives the impurity level to a shallower energetic position.

To test these ideas, we have calculated the electronic structure of  $\text{GaP:N}$  and  $\text{GaAs:N}$  with both unrelaxed and relaxed bonds. EPM calculations on large (4096-atom) cells with both unrelaxed and VFF relaxed geometries show that (Fig. 8) relaxation in  $\text{GaP:N}$  makes the level *deeper*, in contradiction with previous expectations.<sup>71,91</sup> Furthermore, Fig. 8 shows that relaxation in  $\text{GaAs:N}$  raises (reduces) the  $\Gamma$ -like ( $L$ -like) content of  $a_1^{\Gamma L}(1)$ , whereas relaxation in  $\text{GaP:N}$  raises (reduces) the  $\Gamma$ -like ( $X$ -like) character of  $a_1^{\Gamma}(1)$ . In fact, in raising the  $\Gamma$  character, relaxation makes the single nitrogen impurity level dipole allowed (“direct gap”) with respect to transitions from the valence-band maximum (VBM), even though the corresponding transition in pure GaP is forbidden (indirect gap). Our results can be explained by noting that relaxation increases the range of the perturbation potential from “single site” in the unrelaxed case, to a few atomic shells around the impurity after relaxation. This increases the magnitude of the nitrogen-induced perturbation, leading to more extensive interband coupling and a deeper energy level.

### H. Summary of results for isolated nitrogen in GaAs and GaP

Substitutional isolated nitrogen in GaAs and GaP causes strong inward relaxation of its neighboring Ga atoms, thus strongly perturbing the cation-localized conduction states of the appropriate symmetry:  $a_1(\Gamma) + a_1(X_1) + a_1(L_1)$ . This coupling creates both localized, nonhydrogenic impurity

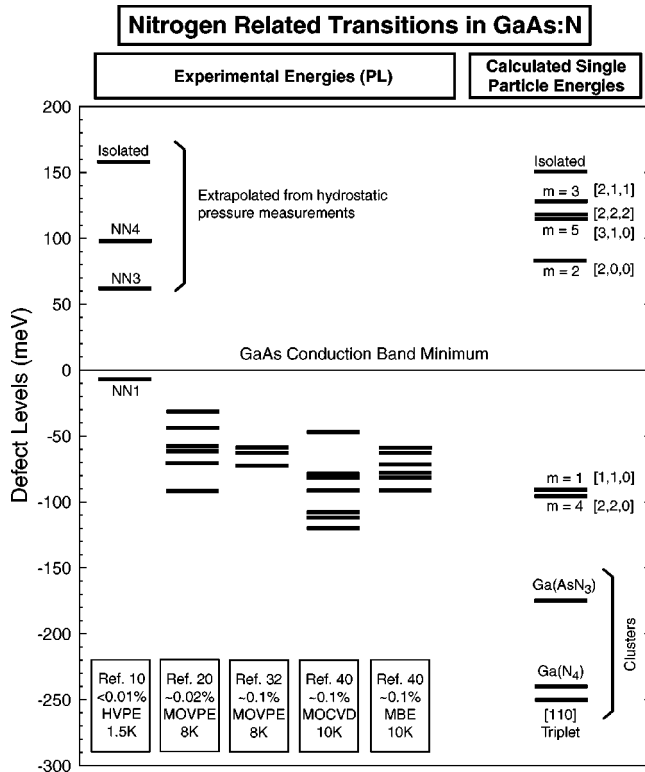


FIG. 9. Experimental and calculated energies of nitrogen-related transitions in  $\text{GaAs}_{1-x}\text{N}_x$ . The peak energy of each transition is shown, for different experiments and samples.

states  $a_1(N)$  and perturbed host states that lead to bowing. In  $\text{GaAs:N}$  the  $a_1(N)$  state is a resonance level above the CBM, whereas in  $\text{GaP}$ , with its  $\sim 0.3$  eV higher CBM, this level appears inside the band gap. Those  $a_1(N)$  levels are characterized by anomalously small pressure coefficients, since they are constructed from the interference of many host bands, not just band-edge states. The lowest perturbed host state (the CBM) is repelled downwards by the other perturbed host states *above* it [not just by  $a_1(N)$  (Refs. 51 and 54)]. This leads to strong alloy bowing and renders  $\text{GaP}_{1-x}\text{N}_x$  “direct gap” by mixing-in  $\Gamma$  character. “Cluster states” within the gap reduce this bowing.

## V. RESULTS: NITROGEN-NITROGEN PAIRS AND HIGHER-ORDER CLUSTERS

Random statistics causes some of the substitutional nitrogen to form  $m$ th nearest neighbors. If we place one nitrogen at the (0,0,0) unit cell position, then the first- to sixth-neighbor nitrogen atoms are located at the lattice positions (1,1,0), (2,0,0), (2,1,1), (2,2,0), (3,1,0), (2,2,2), respectively. Although the number of nitrogen pairs is expected to be only a small fraction of the total nitrogen concentration in dilute alloys, experimental studies conclude that the pairs dominate the emission spectra of these alloys, due to an efficient transfer of excitons to the nitrogen pair levels before emission. Detailed experimental studies on such N-N pairs are available for  $\text{GaP}$  (Refs. 1,92,6,13,93 and 23) and  $\text{GaAs}$  (Refs. 7,10,24 and 81) host crystals. The ensuing observed levels

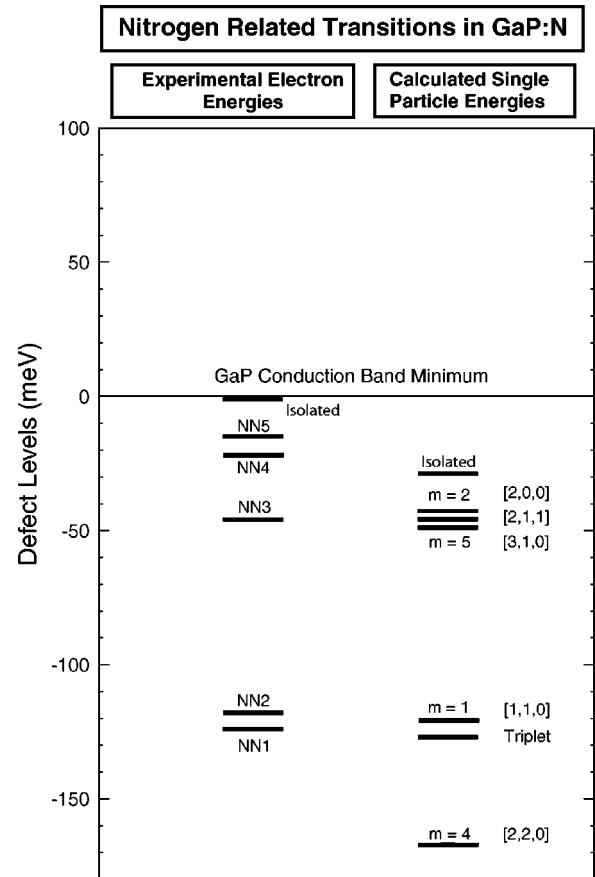


FIG. 10. Experimental and calculated energies of nitrogen-related transitions in  $\text{GaP}_{1-x}\text{N}_x$ . The experimental data is from Ref. 6.

are compiled in Figs. 9 and 10. For  $\text{GaAs}_{1-x}\text{N}_x$  (Fig. 9) the scatter in measured levels is large, and no clear assignment of level to particular pairs has emerged as yet. For  $\text{GaP}_{1-x}\text{N}_x$  (Fig. 10) the situation is clearer.

In  $\text{GaP}$ , experiments reveal a series of sharp luminescence lines, extending from  $\sim 30$  meV to  $\sim 150$  meV below the CBM.<sup>1,92</sup> The levels were originally attributed<sup>1,92</sup> to a first-nearest-neighbor nitrogen pair for the deepest level, to a nitrogen-nitrogen pair of increasing separation corresponding to progressively shallower levels, although this is no longer believed. The series terminates at a level attributed to isolated nitrogen just below the band gap (see Sec. IV).

In  $\text{GaAs}$ , the experimental studies<sup>7,10,24,81</sup> find that, in contrast to  $\text{GaP}$ , the levels due to nitrogen pairs reside principally *within* the conduction band. At zero pressure, for dilute alloys ( $\leq 0.1\%$ ), only a single NN1 line resides inside the band gap.<sup>7,10,24</sup> However, Liu *et al.* demonstrated that under hydrostatic pressure, additional NN lines are forced into the band gap, culminating in the emergence of the isolated impurity line at  $\sim 2$  GPa. More recent experiments for samples of higher nitrogen concentration have attributed levels detected deeper within the band gap at zero pressure<sup>25–27,81</sup> to the formation of nitrogen *clusters*. In this section we will study the calculated energy levels of various assumed pairs and triplets.

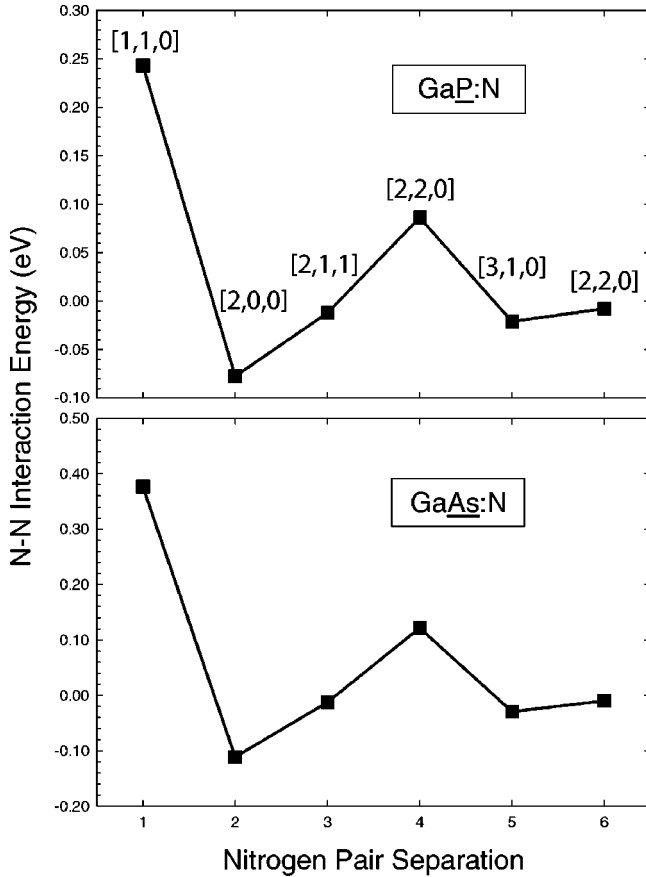


FIG. 11. N-N pair interaction energies for GaP:N calculated using the valence force field method.

### A. Energetics of clustering tendencies in N-N pairs

We first ask whether a pair of infinitely separated ( $m \rightarrow \infty$ ) nitrogen atoms in GaAs or GaP tend to attract or repel each other. We thus estimate the strain energy of  $m$ th-neighbor N-N pairs with respect to the energy of a well-separated ( $m \rightarrow \infty$ ) pair by calculating the interaction energy

$$\Delta E^{(m)} = E(\text{GaP:N}_2^{(m)}) + E(\text{GaP}) - 2E(\text{GaP:N}). \quad (8)$$

Figure 11 shows  $\Delta E^{(m)}$  from valence force field (VFF) calculations for a large (13 824-atom) cell, where the energies are converged. The lattice constant is taken at the Vegard value. We see that the  $m=2$  and  $m=5$  pairs have an attractive strain energy, whereas  $m=1$  and  $m=4$  are strongly repulsive. Although the VFF Hamiltonian excludes the charge-transfer terms necessary to model the rebonding around near-neighbor nitrogen atoms, this data suggests that pair formation is energetically favored clearly for at least for (100)-oriented first neighbors.

To test these conclusions we have also performed LDA calculations with a small 64-atom cell. In GaP, we find that formation of  $m=2$  and  $m=3$  pairs is energetically favored ( $\Delta E^{(m)}$  is negative, by 147 and 172 meV, respectively), while  $m=1$  pairs are unfavorable by 18 meV. In GaAs we find that only  $m=2$  pairs are favorable. As our small LDA supercell is unable to contain the long-range lattice relax-

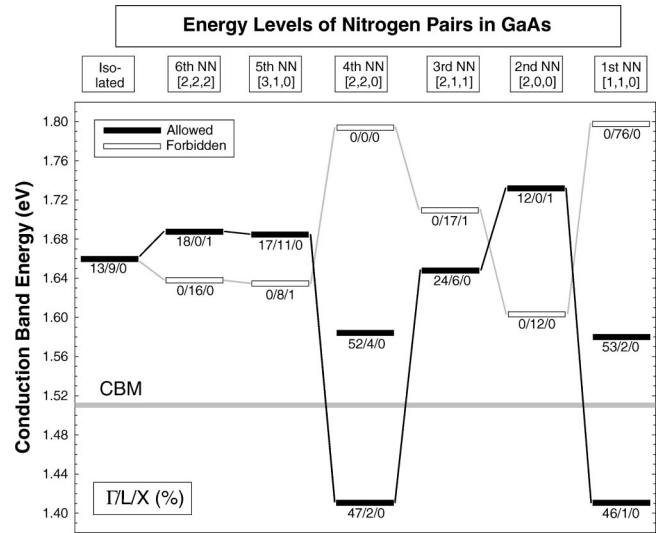


FIG. 12. The energy levels of isolated N and N-N pairs in GaAs. The legend indicates orientation (e.g., [1,1,0]) with respect to one nitrogen at the origin. The allowed (solid bar) or forbidden nature (hollow bar) of transitions to the valence band is indicated and the  $\Gamma$ ,  $L$ ,  $X$  character of each state is shown, computed using the spectral decomposition of Ref. 70.

ation expected for pairs, we predict that LDA calculations in larger supercells will find pair formation increasingly favorable due to the strain relief around the impurity sites.

The attractiveness of the strain interaction for the (100)-oriented ( $m=2$ ) impurity pair is a general feature of the zinc-blende lattice (e.g. it was found<sup>94</sup> for As-As pairs in cubic GaN). Recent scanning tunneling microscopy measurements by McKay *et al.*<sup>95</sup> on 1.7% nitrogen in GaAs revealed that (001)-oriented first neighbors ( $m=2$ ) have a concentration that exceeds the expectations of random statistics. Both experiment and bulk calculation indicate that the distribution of other pairs is close to random statistics. Surface effects<sup>96,97</sup> that are important during vapor-phase growth could change this picture. We conclude that (110)-oriented pairs are less favorable than random statistics whereas (001) pairs are more favored, but all other pairs exist randomly.

### B. N-N pair energy levels and wave functions: Cluster states

Figures 12 and 13 show the calculated energy levels of N-N pairs, in GaAs and GaP, respectively (cell size 4096 atoms). While Fig. 14 shows isosurface plots of the lowest-energy wave function of pairs in GaP (wave functions of nitrogen pairs in GaAs are visually similar). Figure 14(a) shows the nitrogen localized isolated impurity level,  $a_1^N(1)$  for reference [see also Fig. 4(a)].

Our results show that the interaction of pair nitrogens results in the formation of a series of “bonding” and “antibonding” states, as expected by the interaction of isolated impurity levels. We have classified the levels as either dipole allowed (from the VBM) or dipole forbidden according to the computed degree of  $\Gamma$  character in the wave functions.<sup>58</sup> Allowed states are shown as black bars in Figs. 12 and 13. Relaxation of atomic positions, neglected in previous

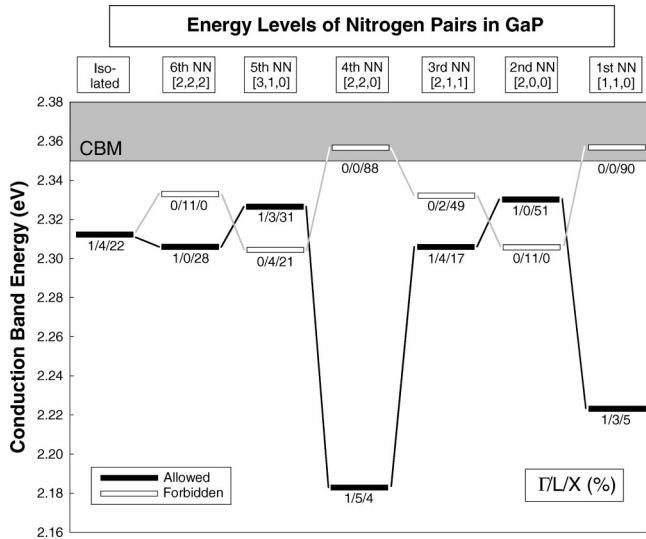


FIG. 13. The energy levels of isolated N and N-N pairs in GaP. Details as per Fig. 12.

calculations,<sup>87,79</sup> can greatly change the oscillator strengths of certain transitions: for example, the unrelaxed isolated nitrogen in GaP has negligible  $\Gamma$  character (almost forbidden), but gains  $\Gamma$  character (strongly allowed) on relaxation. Figures 14(b)–14(f) illustrate the formation of “bonding” states at small nitrogen-nitrogen separation. At large separation, e.g. fifth-nearest-neighbor positions [Fig. 14(b)], the pair wave functions resemble those of two isolated nitrogens, while at small separation, e.g., first-nearest-neighbor positions [Fig. 14(f)] show bonding character with significant charge density *between* the nitrogens.

In GaP, the lowest energy level of each nitrogen pair resides within the gap, while for GaAs only the first- and fourth-nearest-neighbor pairs create gap levels. This disparity, as for the isolated impurity, results primarily due to the conduction-band lineup of GaAs and GaP compared to GaN (Sec. IV D and Fig. 1). We note in Figs. 12 and 13 that (110)-oriented nitrogen pairs (first and fourth neighbors) are particularly deep both in GaP and GaAs. A structural feature of the zincblende lattice is that atoms are connected to each other only through the (110)-oriented zig-zag chains. When two arsenic atoms are replaced by nitrogen along this chain, the short (1.95 Å) Ga-N bond replacing the longer (2.45 Å) Ga-As bond causes the adjacent Ga atoms to interact. The combined electronic and geometric interaction is evident in the wave functions of the  $m=1$  and  $m=4$  pairs, shown in Figs. 14(f). In both cases wave-function localization is evident *along* the (110) chain. We will see in Sec. V C that longer chains along the [110] direction lead to even deeper states within the gap.

We also calculated the energy levels for a first-nearest-neighbor pair of indium atoms in GaAs. No gap states were created, in contrast to the nitride alloys, due to the smaller differences in atomic size.

Our calculated pair levels are clearly a nonmonotonic function of pair separation. The final energy levels result from a combination of multiband coupling and lattice relaxation around the nitrogen impurities. By performing both relaxed and unrelaxed calculations, and by comparing with simpler calculations,<sup>87,79</sup> we have found that both effects—multiband coupling and lattice relaxation—are critical to reproducing the nitrogen pair levels. One or both of these ef-

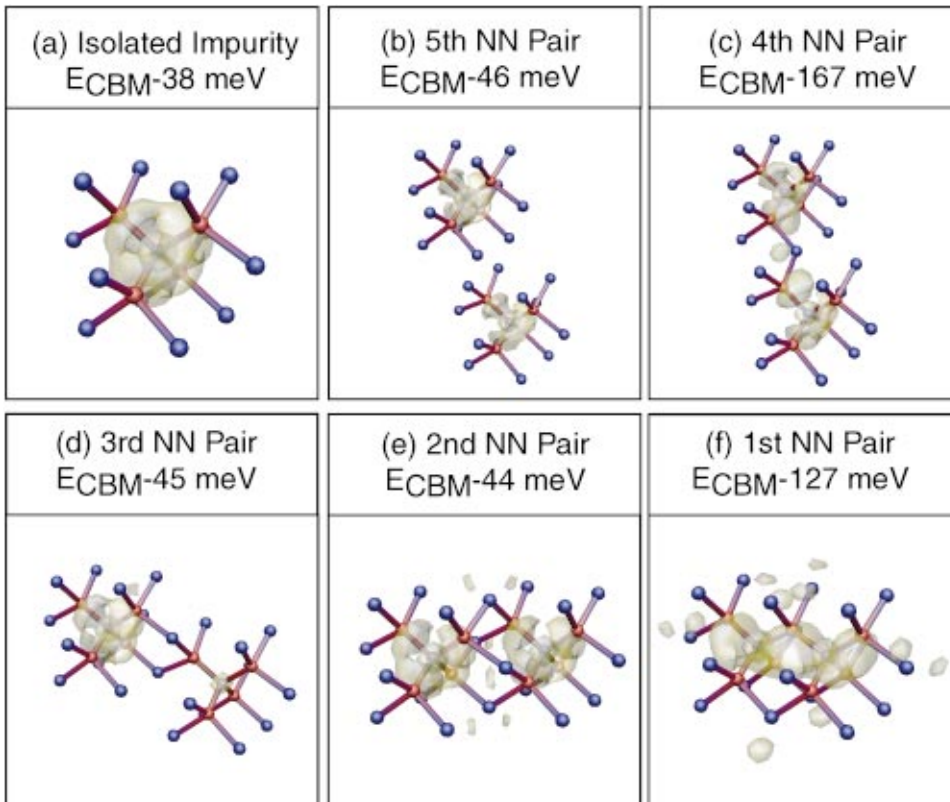


FIG. 14. (Color) Wave function isosurfaces (yellow) of isolated N and N-N pairs in GaP. The nitrogen impurities are shown (black), and, for simplicity, only the neighboring gallium atoms are depicted (red). Isosurfaces are drawn at 20% of maximum (supercell size: 4096 atoms).

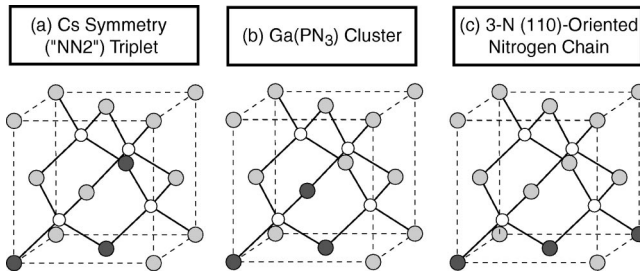


FIG. 15. Geometries of nitrogen triplets: (a)  $C_s$  symmetry triplet, ascribed to the NN2 line in GaP:N, (b) GaPN<sub>3</sub> cluster, of three nitrogens around a single gallium atom, and (c) (110)-oriented triplet.

facts has been neglected in many previous calculations<sup>87,79,98,99</sup> of the pair levels, explaining the large variance of results between them. Earlier calculations have also collated the pairs into similarly oriented groups,<sup>87,100,79</sup> e.g., pairs on the [110] axis, and predicted a monotonic ordering of energy levels for pairs within each group. However, we find this is not the case as we find a nonmonotonic ordering even for similarly oriented pairs: in GaP a fourth-neighbor pair is lower in energy than a first-neighbor pair for both relaxed (Fig. 13) and unrelaxed lattices. This analysis shows that multiband coupling alone produces a nonmonotonic ordering.

### C. Higher nitrogen aggregates and cluster states

#### 1. Nitrogen triplets

Uniaxial pressure measurements of GaP:N (Ref. 93) have demonstrated that the photoluminescence lines historically associated with nitrogen pairs cannot, in fact, be solely due to pairs. These lines have historically been labeled as NN1, NN2, and so on, starting with NN1 as the deepest level.<sup>1</sup> In fact, except for the NN1, NN3, and NN4 lines, the stress-induced splitting cannot be assigned to  $m$ th nearest-neighbor pairs.<sup>93</sup> These results suggest that the other NN lines may be due to triplets and other small nitrogen aggregates.

The NN2 line is an important discrepant example as it occurs early in the NN spectrum. Although previously associated with a second-nearest-neighbor pair,  $m=2$ , under uniaxial pressure the NN2 line demonstrates an  $C_s$  compatible symmetry,<sup>93</sup> while a second nearest neighbor pair has  $D_{2d}$  symmetry. Gil and Mariette<sup>101</sup> proposed a N-N-N triplet structure, depicted in Fig. 15(a), as a probable candidate for the NN2 line. This structure consists of the [110] pair plus a third atom at [210]. We have calculated the electronic structure of this structure. We find this triplet has a dipole allowed level 41 meV above our calculated deepest pair level (the NN1 line), and a calculated pressure coefficient of 26 meV/GaP, in close agreement with experimental value of 21 meV/GPa.<sup>13</sup> This supports the model proposed by Gi and Mariette.

#### 2. Ga-centered clusters and [110] chains

As further examples of nitrogen clustering we have considered nitrogen clusters centred around single Ga atoms.

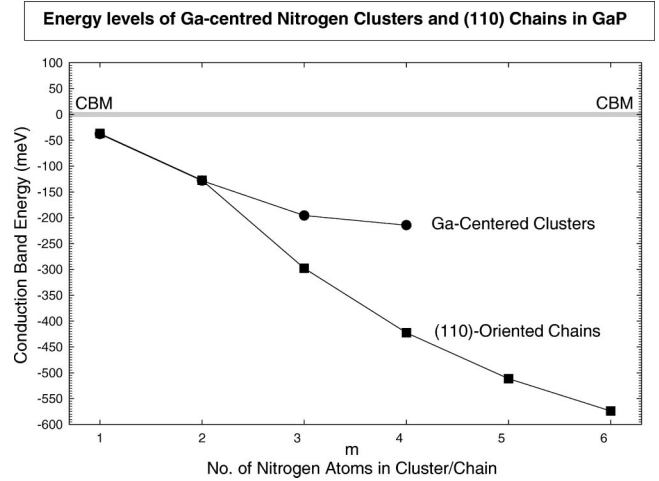


FIG. 16. Energy levels of Ga-centered nitrogen clusters and (110)-directed nitrogen chains in GaP, calculated in 4096-atom cells.

The Ga-centered tetrahedron in GaP<sub>1-x</sub>N<sub>x</sub> can have its four vertices occupied by P<sub>4-p</sub>N<sub>p</sub>, with  $0 \leq p \leq 4$ . In GaAs<sub>1-x</sub>N<sub>x</sub> we can have Ga(As<sub>4-p</sub>N<sub>p</sub>). (Note that  $p=2$  is  $m=1$  of Figs. 12 and 13.) We show a  $p=3$ , Ga(PN<sub>3</sub>) cluster in Fig. 15(b). Figures 16 and 17 show the energies of these “cluster states” for different  $p$  values for GaP and GaAs, respectively. In these calculations we have embedded a single cluster in a 4096-atom supercell. We see that the levels become deeper as  $p$  increases, consistent with the fact that on an absolute scale the CBM of GaN is  $\sim 0.5$  eV below that of GaAs.

We also considered extended [110]-oriented chains of increasing length. Figure 15(c) depicts a three-nitrogen [1,1,0] chain. Our calculated energy levels are shown in Figs. 16 and 17. With 3,4,5 etc., nitrogen atoms we found that each additional atom in the chain produced successively deeper levels. All are dipole allowed. Despite the high strain of these structures, these energy levels suggest that the long “low-energy tail” observed at the conduction-band edge of

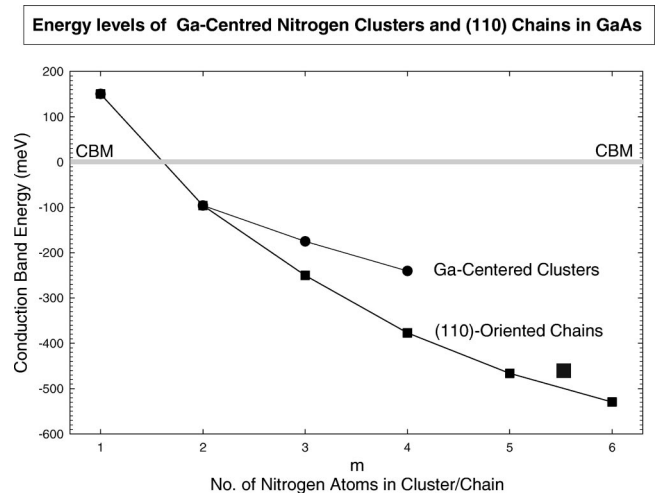


FIG. 17. Energy levels of Ga-centered nitrogen clusters and (110)-directed nitrogen chains in GaAs, calculated in 4096-atom cells.

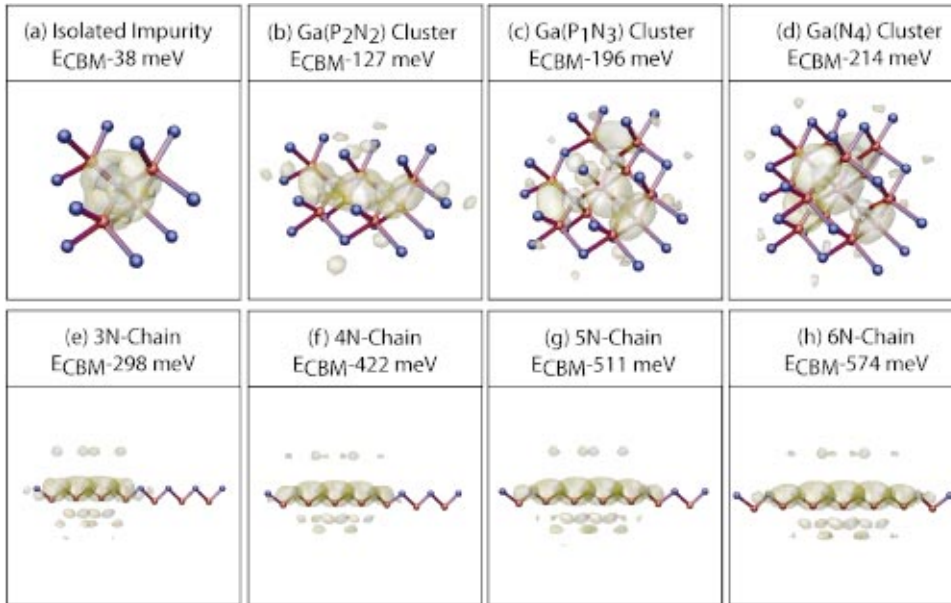


FIG. 18. (Color) Wave function isosurfaces (yellow) of cluster states at (a)–(d) Ga-centered nitrogen clusters  $\text{Ga}(\text{P}_{4-m}\text{N}_m)$ ,  $1 \leq m \leq 4$ , and (e)–(h)  $[110]$ -directed nitrogen chains in GaP, calculated for 4096-atom cells. The nitrogen impurities are shown (black), and, for simplicity, only the neighboring gallium atoms are depicted (red).

currently grown high-nitrogen-content samples<sup>102,33,103</sup> may be due to short chains of nitrogen atoms or similar nitrogen aggregates. Note that the  $[110]$  chain states are deeper than Ga-centered clusters for three and four nitrogen atoms (Fig. 16) due to the large uniaxial strains along the chains.

Figure 18 shows the lowest-energy wave functions for the different cluster and chain geometries considered in GaP. Figures 18(a)–18(d) depict the wave functions of  $\text{Ga}(\text{P}_{4-p}\text{N}_p)$  clusters, showing the strong localization around the central Ga atom due to the formation of a GaN-like region. Figures 18(e)–18(h) depict the  $[110]$ -axis localization resulting from  $[110]$  nitrogen chains.

Recent photoluminescence measurements of  $\text{GaP}_{1-x}\text{N}_x$  alloys have indicated the present deeper levels in samples with  $x_N \geq 0.43\%$ .<sup>33</sup> The data show the presence of a new deep level (labeled “NC” in Ref. 33 at 2.071 eV, which is deeper than both the calculated nitrogen pair and Ga-centered cluster levels). Figure 16 shows that this observed center might be the three-membered  $[110]$  chain depicted in Fig. 15(c) (which can also be thought of as two first-neighbor pairs). This structure introduces a single gap level, calculated at  $\sim 2.059$  eV, in good agreement with the experimental data. We therefore tentatively identify the NC level<sup>33</sup> as an  $[110]$ -oriented triplet of  $C_{2v}$  symmetry.

#### D. Summary of results on nitrogen clusters

Random incorporation of N in III-V compounds leads to the formation of nitrogen pairs and higher clusters.  $(001)$  pairs are energetically most favorable, whereas  $(110)$  pairs are least favorable. The pairs introduce levels in the gap whose energy varies nonmonotonically with pair separation. The deepest states are the  $(110)$ -oriented pairs. When these pairs form into  $(110)$ -oriented chains, deeper levels result, reflecting highly-localized due to interactions along the close-packed  $(110)$  chains of the zinc-blende structure. For comparison, chains of In in GaAs do not form localized levels. The levels introduced by chains are highly localized, have

low pressure coefficients, and are connected to the VBM by dipole-allowed (direct) transitions.

We offer particular clusters as tentative models for observed deep PL by Zhang *et al.*<sup>33</sup> and by Gil and Mariette,<sup>101</sup> but the complexity of the predicted pair, chain and higher cluster states for higher nitrogen concentrations precludes any definitive assignment of the many observed PL lines. The reasons that contribute to differences between our calculated energy levels and the experimental energies include a lack of electronic relaxation upon excitation, and a lack of many-body corrections to the single-particle energies. Despite this, the EPM gives a correct overall account, with the isolated impurity shallowest, pairs deeper, and (yet unmeasured) clusters deeper still.

## VI. RESULTS: ALLOY PROPERTIES

### A. Why is the alloy valence band maximum split?

The foregoing discussion indicates that the introduction of a single N-N pair or N-N-N-triplet in a zinc-blende lattice lowers the global symmetry. Hence, symmetry-mandated degeneracies of the zinc-blende structure will be removed. It is interesting to inquire about the size of the splitting for a given concentration.

We have thus taken a 1000-atom GaAs supercell containing randomly distributed nitrogen atoms, calculating the electronic structure for  $\sim 15$  different, randomly selected, configurations for several compositions. We find average splittings among the valence-band maximum states of 3(2), 6(3), 20(17), and 27(29) meV at  $x_N = 1, 2, 3,$  and 4%, respectively, where our splittings are defined as the energy difference between the uppermost and lowest VBM levels (first and third, excluding spin-orbit), and the configuration level spread (standard error) is given in parentheses. For nitrogen concentrations  $x \leq 2\%$ , the splittings increase approximately linearly with concentration, as the impurities only weakly perturb the host VBM. For greater concentrations, the mag-

nitude of the splitting sharply increases due to the increased probability of cluster formation in the nascent alloy. The fluctuations in the splittings increase concomitantly (evidenced by larger statistical spread compared to low concentrations) reflecting the strong dependence on pair, triplet, and cluster orientation within the alloy. The strong fluctuations observed here will be reflected in actual  $\text{GaAs}_{1-x}\text{N}_x$  samples: measured valence-band splittings will be strongly affected by the degree of clustering and short-range order within each sample. Orientational averaging over pairs is expected to broaden these features and eventually average them out.

The clustering-induced splitting  $\Delta_{\text{CS}}$  at the valence-band maximum results from lifting of the cubic symmetry of GaAs by the nitrogen clusters in the film. This source of splitting should be distinguished from the film/substrate mismatch strain effects  $\Delta_\epsilon$ , proportional to the misfit strain  $\epsilon_\perp = (a_{\text{GaAs}} - a_{\text{GaAs}_{1-x}\text{N}_x})/a_{\text{GaAs}}$  between the  $\text{GaAs}_{1-x}\text{N}_x$  film grown on a GaAs substrate. For (001) growth direction we have

$$\Delta_\epsilon = -2b\epsilon_\perp(1 + 2C_{12}/C_{11}), \quad (9)$$

where  $b$  is the biaxial deformation potential and  $C_{ij}$  are elastic constants. The total measured splitting  $\Delta$  is then  $\Delta \approx \Delta_{\text{CS}} + \Delta_\epsilon$ . It was found<sup>104</sup> that the total measured splitting for  $\text{GaAs}_{1-x}\text{N}_x/\text{GaAs}(001)$  was  $\Delta \approx 24\text{--}62$  meV for  $x = 1.1\text{--}3.3\%$ , which is larger than the range of  $16\text{--}53$  meV expected from film/substrate strain, Eq. (9), using the value  $b = -1.9$  eV of GaAs. In fact, a larger value of  $b$  was necessary to fit the total measured splitting in  $\text{GaAs}_{1-x}\text{N}_x$  to Eq. (9), prompting the conclusion<sup>104</sup> that nitrogen alloying anomalously alters the response of the valence band to biaxial strain. We note, however, that part of the total measured splitting could well be due to clustering-induced splitting, so only  $\Delta - \Delta_{\text{CS}}$  must be fit to Eq. (9) to extract  $b$ . Our calculated  $\Delta_{\text{CS}}$  is close to the amount by which the measured splitting overestimates the values expected from film/substrate splitting alone. Thus, the ensuing biaxial deformation  $b$  is then less anomalous than hitherto assumed, in Ref. 104.

### B. Pressure dependence of $\text{GaP}_{1-x}\text{N}_x$ transitions

We have already seen (Sec. IV C) that for the isolated impurity in GaP the pressure dependence of the gap level is very small compared to the bulk, and we now consider the pressure dependence of the *alloy* band gap. In earlier pseudopotential calculations it was noted<sup>58</sup> that in  $\text{GaP}_{1-x}\text{N}_x$  the CBM is made of a mixture of the  $X_{1c}$  level and localized impurity states. The pressure coefficient of the CBM was not calculated in that work. Shan *et al.*<sup>54</sup> deduced from this that the predicted pseudopotential pressure coefficient of the CBM would be negative (characteristic of bulk  $X_{1c}$  states) in contrast with their measured data. Our pseudopotential calculations (Fig. 7) show that the calculated pressure coefficient for the 1–3% alloy is in fact strongly positive, in the range  $15\text{--}40$  meV/GPa and agrees quantitatively with the experimental data.<sup>54</sup> Thus, the off- $X_{1c}$  character mixed into the CBM leads to an overall positive pressure coefficient in

agreement with experiment. As nitrogen composition increases there are more nitrogen pairs and other clusters. Their energies move progressively deeper into the gap, i.e., to lower PL energies. Such clusters have large  $\Gamma$ - $X$  mixing (larger pressure coefficients), since they represent increasing perturbations on the single substitutional impurity. Thus, the pressure coefficient increases as the PL energy decreases or composition increases. The overall positive pressure coefficient for the  $\text{GaP}_{1-x}\text{N}_x$  alloys is in marked contrast to the isolated nitrogen impurity in GaP, where both the calculated and measured<sup>13</sup> pressure coefficients are  $\pm 1$  meV/GPa; it is the pair states (and consequent mixing) that are responsible for the large positive pressure coefficient of the alloy.

### C. Is the $\text{GaP}_{1-x}\text{N}_x$ alloy direct or indirect gap?

Usually, alloys whose binary components are of opposite optical response (e.g., direct gap GaAs and indirect gap GaP) exhibit an abrupt, first-order direct-indirect transition as a function of composition. Early measurements<sup>59</sup> suggested such a transition at 48% nitrogen in  $\text{GaP}_{1-x}\text{N}_x$ , but calculations by Bellaiche *et al.*<sup>58</sup> predicted a direct-gap behavior already at 3% nitrogen. Shan *et al.*<sup>54</sup> noted that, experimentally, the transition between valence and conduction band in  $\text{GaP}_{1-x}\text{N}_x$  is allowed already at a composition of 0.7% and suggested that this might be in conflict with the earlier calculations.<sup>58</sup> Figure 5 shows that our calculation predicts an incorporation of  $\Gamma$  character into the  $\text{GaP}_{1-x}\text{N}_x$  conduction band *already* for the lowest nitrogen concentration calculated (in Bellaiche *et al.*<sup>58</sup> the lowest calculated was 3%, here it is 0.01%), in agreement with experiment.<sup>13,93,23</sup> Our data predict that adding any amount of nitrogen impurities in GaP can be considered as adding “direct gap” ( $\Gamma$ ) character to the material. Note therefore that there is no indirect to direct (first-order) “transition” (e.g., as in  $\text{GaAs}_{1-x}\text{P}_x$ ), but a gradual increase in  $\Gamma$  mixing into the CBM, starting from the lowest nitrogen incorporation. This is in sharp contrast with the prediction of Baillargeon *et al.*<sup>59</sup> and Sakai *et al.*,<sup>105</sup> suggesting an indirect to direct *transition* at  $\sim 48\%$  nitrogen.

## VII. EVOLUTION OF $\text{GaAs}_{1-x}\text{N}_x$ AND $\text{GaP}_{1-x}\text{N}_x$ ALLOY STATES WITH NITROGEN COMPOSITION

### A. Electronic structure evolution

We have shown that nitrogen introduces two types of states in the dilute limit: (i) the perturbed host states (PHS) residing within the continuum such as  $a_1(X_{1c})$ ,  $a_1(L_{1c})$ , and  $a_1(\Gamma_{1c})$ , and (ii) The cluster states (CS) residing inside (or near) the band gap, e.g., the pair and higher cluster states. We next address the question of how the PHS and CS evolve as the nitrogen composition increases.

One can envision at least two scenarios: if the CS have sufficiently extended wave functions so as to overlap other clusters, the primary interaction will be between different cluster states, i.e., a CS-CS interaction. Their energy will then shift with concentration, forming their own “impurity band” just as large-orbit effective-mass impurities do<sup>35</sup> (e.g., phosphorus in silicon). If, on the other hand, the CS have localized wave functions but the PHS have extended wave

functions, the primary interaction could be between CS and PHS. To decide between these possibilities one needs to know the localization of the relevant wave functions. Since the CS are manifestly nonhydrogenic centers (i.e., their wave function mixes bands throughout the Brillouin zone), we can not estimate their spatial extent of the wave function from simple effective-mass formulas involving a single band, but a full calculation is needed. This is our next task.

We perform calculations as a function of nitrogen concentration, by randomly distributing up to 20 nitrogen atoms onto the anion sites of GaP and GaAs of a 1000-atom supercell (i.e.,  $x_N=4\%$ ). We relax the atomic positions and calculate the electronic structure, repeating this for 15 randomly selected configurations at each composition to establish a statistically representative sample. The ensuing energy levels are then collected and analyzed for their degree of localization, by computing for each level  $\psi_i$  the distance  $R_\alpha^{(i)}$  from the  $\alpha$ th nitrogen site at which 20% of the wave function is enclosed. Through this measure we have classified each level as either “localized” or “quasilocalized” for (CS) and PHS, respectively.

### 1. Evolution of alloy states in $\text{GaP}_{1-x}\text{N}_x$

Figure 19 depicts the spectral dependence of the average localization  $\Sigma_\alpha(1/R_\alpha^{(i)})$  for localized and quasilocalized levels of  $\text{GaP}_{1-x}\text{N}_x$ . Panel (a) shows the localized single-impurity  $a_1(N)$  state, selected pair, and triplet and quadruplet [ $\text{GaP}(\text{N}_3)$  and  $\text{Ga}(\text{N}_4)$ ] cluster states, appearing inside the band gap. These wave functions are highly localized. Panel b shows the more extended perturbed  $X$ ,  $L$ , and  $\Gamma$  host states, and the edge of the conduction band, denoted by the bold arrow “ $E_{\text{CBE}}$ .” As the nitrogen concentration increases, Figs. 19(d,f,h,j) show that the edge  $E_{\text{CBE}}$  of the conduction-band minimum (vertical heavy arrow) moves rapidly to lower energies, due to anticrossing and repulsion with higher-energy members of the PHS. At the same time, the energy of the CS are pinned and remain fixed, as these highly localized states do not strongly interact with each other. Indeed the wave function of the CS do not change with composition. As the edge of the PHS moves rapidly to lower energies (“optical bowing”) this broad band of states sweeps past the discrete CS one by one. At a critical composition  $x_c$  (which depends on the degree of randomness in the samples), the deepest CS is overtaken by the moving PHS. Near  $x_c$ , the conduction-band minimum is an “amalgamated state” formed [Fig. 20(b)] from both semilocalized (Fano-resonance-like) states (shown in red isosurfaces) and more delocalized parts (shown as green isosurfaces). As we will see below, this duality in the amalgamated state can lead to unusual physical effects. For higher nitrogen concentrations exceeding  $x_c$  [Fig. 19(g)], the CS are well inside the conduction band, and the states near the edge are more extended [Fig. 20(c)].

### 2. Evolution of alloy states in $\text{GaAs}_{1-x}\text{N}_x$

Figure 21 shows the evolution of the  $\text{GaAs}_{1-x}\text{N}_x$  states as a function of composition. We see that as the conduction band edge (CBE, also called “ $E_-$ ”) plunges *down in energy*

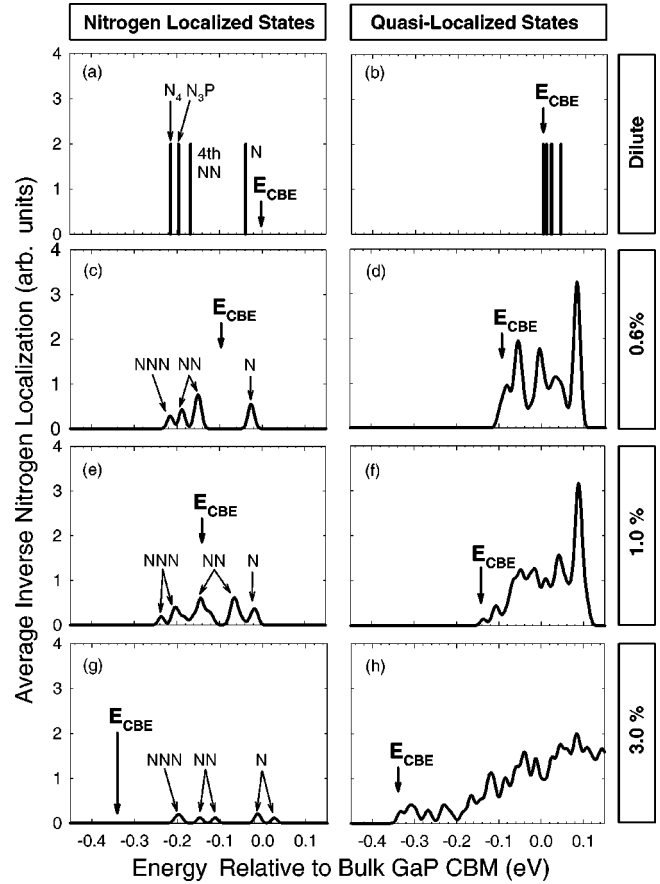


FIG. 19. Spectral dependence of average nitrogen localization for (left) nitrogen localized cluster states and (right) quasilocalized perturbed host states of  $\text{GaP}_{1-x}\text{N}_x$  for selected nitrogen concentrations. States with at least 20% of total charge within 4.1 Å radius of any nitrogen atom are classified as nitrogen-localized. The vertical arrows show the position of the alloy conduction-band edge  $E_{\text{CBE}}$ .

as  $x_N$  increases, sweeping past the most localized cluster states already by  $x \sim 0.6\%$ . At the same time the  $t_2(L_{1c})$  band appears constant in energy, at  $E_c + 0.4$  eV, while the upper edge of the PHS [also called  $E_+$  (Ref. 51)] appears for  $x \sim 0.6\%$  and moves *up in energy* as  $x_N$  increases. This broad band represents mostly delocalized or weakly localized  $a_1$  perturbed host states.

We have previously noted<sup>62</sup> that in  $\text{GaAs}_{1-x}\text{N}_x$  the  $L_{1c}$  level of pure GaAs splits into  $t_2(L_{1c}) + a_1(L_{1c})$  and that the  $a_1(L_{1c})$  mixes in with the localized impurity level. Shan *et al.*<sup>55</sup> deduced from this that our model will predict that N perturbs the  $E_1$  interband transition (which includes  $L_{1v} \rightarrow L_{1c}$  contributions), in contrast with their data for the interband transition near 3 eV, which are composition independent. However, the  $E_1$  transition encompasses a large volume in the Brillouin zone, not just the  $L$  point. Our calculated  $L$ -like  $t_2$  peak in the conduction band at  $E_c + 0.43$  eV in Fig. 21 is seen to be composition independent. The transition between  $L_{1v}$  and  $L_{1c}$  states at  $\sim 3$  eV ( $L_{1v}$  is at  $E_v - 1$  eV, the gap is 1.5 eV, and  $L_{1c}$  is at  $E_c + 0.43$  eV) is therefore predicted to be only weakly affected by nitrogen composition as seen experimentally.<sup>55</sup> The  $a_1$  component of  $L_{1c}$  may be difficult to detect as it hybridizes with the broader  $a_1$ -like

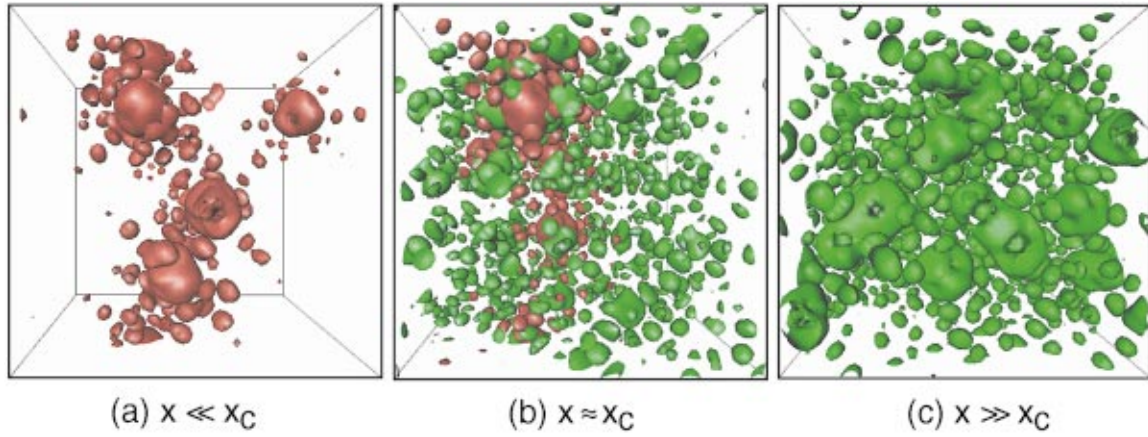


FIG. 20. (Color) Isosurfaces of the conduction wave functions for (a)  $x \ll x_c$   $\text{GaAs}_{1-x}\text{N}_x$  showing nitrogen-localized cluster states within the gap (red), (b)  $x \approx x_c$  showing the “amalgamated state” of localized (red) and the delocalized (Bloch-like) states (green), and (c)  $x \gg x_c$  extended states (green).

PHS band. Between  $E_+$  and  $E_-$  we observe a broad band of states whose character is  $L$ -like.

### B. The three regions of alloy behavior

We can now divide the alloy evolution with  $x_N$  into a few regimes with distinct behavior.

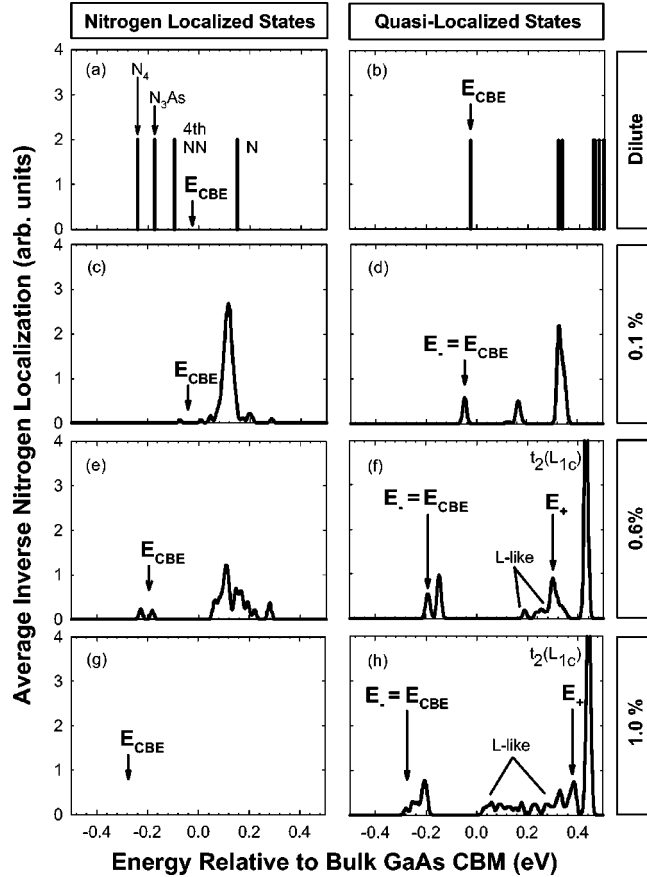


FIG. 21. Spectral dependence of average nitrogen localization for (left) nitrogen localized cluster states and (right) quasilocalized perturbed host states of  $\text{GaAs}_{1-x}\text{N}_x$  for selected nitrogen composition. Other details as per Fig. 19.

(a) *The dilute alloy* ( $x \ll x_c$ ). In this regime the conduction band consists of nitrogen-perturbed host states  $a_1 + e + t_2$  inside the conduction continuum, as well as cluster states inside the band gap. The cluster wave functions are very localized (Figs. 3 and 4). Absorption takes place to the PHS and the  $a_1(N)$  states, whereas emission takes place from the lower-energy CS inside the band gap. With increasing temperature, the CS are thermally depopulated, leading to a large redshift of the band gap with temperature. The pressure dependence of the emission from the CS is very small relative to the band edge of the pure host (see Figs. 6 and 7), as these CS are highly localized and weakly coupled to the host states. As pressure increases, the  $\Gamma_{1c}$  state of GaAs moves up faster than the CS, thus exposing the  $a_1(N)$  state of GaAs:N as a gap state above  $\sim 2$  GPa. For  $\text{GaP}_{1-x}\text{N}_x$ , the pressure coefficient of the CS in the dilute limit is less negative than that of the downward moving GaP  $X_{1c}$  edge, so the impurity level becomes shallower as pressure increases. The pair states have a positive pressure coefficient. The admixture of  $\Gamma_{1c}$  character, however, makes the CS of  $\text{GaP}_{1-x}\text{N}_x$  “direct gap.”

(b) *The intermediate region*  $x \approx x_c$ . Here, the conduction-band edge is formed from the delocalized PHS and some localized CS. In this regime one observes exciton localization due to the CS potential fluctuations. The exciton lifetime is thus rather long.<sup>36</sup> The effective mass at the bottom of the band is larger than that of GaAs ( $m^* = 0.067$ ), as heavy-mass  $X_{1c}$  and  $L_{1c}$  character is mixed in. As one moves the Fermi energy deeper into the conduction band via  $n$ -type doping, the effective mass becomes even heavier, as more resonant CS are encountered. For concentrations  $x_N = 2-4\%$  in GaAs we calculate a continued gradual decrease in the degree of  $\Gamma_{1c}$  character at the conduction-band edge. This suggests that the alloy electron effective mass continues to increase (to a few multiples of the GaAs effective mass). The temperature dependence of the band gap is reduced relative to GaAs, since the mixed-in localized CS carry a lower temperature coefficient than the extended GaAs states. The pressure dependence of the band edge states is slightly higher than in the isolated impurity limit, as more delocal-

ized states ( $\Gamma, L$ ) are mixed into the localized states. For  $\text{GaP}_{1-x}\text{N}_x$ , the band gap pressure coefficient is no longer weak ( $\sim 0$ ) as in the isolated impurity case, but is strongly positive. In  $\text{GaAs}_{1-x}\text{N}_x$  we observe in this composition range the development of a broad  $E_+$  band that shifts up with composition while the  $t_2(L_{1c})$  states is fixed.

(c) *The high concentration  $x \gg x_c$  limit:* While electronic structure calculations can be made in this concentration limit, in practice, actual limitations in nitrogen solubility in III-V compounds prohibit one from getting stable homogeneous samples. The properties of experimental samples in this limit are critically determined by the degree of clustering or phase decomposition. It is interesting to consider what the electronic properties in this regime would be. Assuming a continued random distribution of nitrogen, our calculations predict the continued large downward bowing of the band gap with increasing nitrogen concentration. In the present work, for  $x_N \sim 50\%$ , we find that bowing is sufficient to close the band gap (in earlier work, we found a small gap,<sup>58</sup>  $\sim 0.2$  eV). Band-gap closure for  $x_N \geq 12\%$  has also been predicted for In-Ga-As-N, the exact concentration depending on the chosen substrate.<sup>106</sup>

### C. Scaling of the band gap

Parametrizing the change in band gap as  $\Delta E \propto x^\alpha$ , we find, for  $\text{GaAs}_{1-x}\text{N}_x$  with many nitrogens,  $\alpha = 0.66$  compared with the experimental value of  $\alpha \sim 0.66$ .<sup>48,57,89,107</sup> It is interesting to enquire whether  $\alpha \ll 1$  results from the existence of impurity clusters, as suggested recently.<sup>90</sup> Indeed, Zhang *et al.* noted that in GaAs:Si where the Si atoms are thought to be isolated,  $\alpha = 1/3$ , and rationalized that in GaAs:N, where pairs exist, one should find  $\alpha = 2 \times 1/3 = 2/3$ . While our calculation does give  $\alpha = 2/3$  when pairs, triplets and other clusters exist, we find that when only one nitrogen is placed in a supercell and the supercell size is changed, there already is an anomalous  $\alpha = 0.76$  (Sec. IV F). Thus, pairs are not needed to get anomalous  $\alpha$ . Furthermore, changing the pseudopotential of nitrogen from that used here to that used in Ref. 63 changes  $\alpha$  from 0.66 to 0.89. Thus,  $\alpha$  is decided by the details of the potential *not by geometric features* (e.g., single versus double impurities). Our analysis shows that  $\alpha < 1$  exists when there are impurity levels near the CBM that couple, potentially slowing down the band gap bowing. The magnitude of this effect depends on the coupling strengths, not on the existence of pairs.

### D. Comparison with the two-level anticrossing model

The two-level model<sup>51</sup> and our alloy model calculations agree on the following points: (i) the  $E_-$  level moves down and the  $E_+$  level move up as  $x_N$  increases (Fig. 21). (ii) The pressure coefficient (reduced with respect to the bulk) saturates as  $x_N$  increases. (iii) N incorporation raises the electron effective mass at the bottom of the CBM, and if one moves further up in energy into the conduction band, the mass increases even further. (iv) the  $E_1$  transition at  $\sim 3$  eV is unaffected by nitrogen. (v) Incorporation of N in GaP reverses the pressure coefficient of GaP to a strongly positive value (Fig. 7), and makes the interband transition direct.

The two models disagree on several issues: (1) Our polycrystalline model includes alloy fluctuations via the existence of many different local environments around nitrogen atoms, giving rise to pairs, triplets, etc. These fluctuations are entirely absent from the two-level model. The fluctuations lead to exciton localization, Stokes-like shift between absorption and emission, *blueshift* with increasing temperature at low temperatures, and to the creation of a localized-to-delocalized transition at the amalgamated point  $x_c$ . (2) Our model shows clearly that more than two levels are perturbed by nitrogen incorporation, e.g., the  $L_{1c}$  and  $X_{1c}$  host states (Fig. 5). This leads to the formation of a wide band of states above  $E_-$  and below  $E_+$  (Fig. 21) that is entirely absent from the two-level model. The mixing in of  $L$  character is evident experimentally, both in the resonant Raman scattering of Cheong *et al.*,<sup>52</sup> and in the BEEM experiment of Kozhevnikov *et al.*<sup>56</sup> (Sec. IV) which directly detected the  $L$  character. (3) For  $\text{GaP}_{1-x}\text{N}_x$ , the two-level model is forced to attribute alloy bowing to the downward shift of the *impurity* states, rather than to the proper alloy conduction band that lies above it.

### E. What are the differences between GaAsN, GaPN, and “conventional” III-V alloys?

We find the following 3 differences.

(1) All common-cation alloys such as  $\text{GaAs}_x\text{P}_{1-x}$  and  $\text{ZnSSe}$  exhibit cation displacement and therefore additional coupling between the cationlike conduction  $a_1$  levels. However the cation displacements are unusually large in common-cation nitrides. Thus, the PHS's  $X_{1c}$ ,  $L_{1c}$ , and  $\Gamma_{1c}$  are more strongly perturbed than in conventional alloys. This leads to larger bowing and more intervalley coupling in nitrides, even in the absence of cluster states.

(2) The large differences between the orbital energies of nitrogen (a first-row atom) and P or As lead to the formation of gap (or near-gap) states even for isolated nitrogen impurities. This is in contrast to P:As or S:Se substitution. These “cluster states” in the gap lead to new phenomenology with respect to alloys that have no CS.

(3) Nitrides show [110]-oriented chain states, whereas most other alloys do not. This is because the small size of the nitrogen atoms permits the cations approach each other much closer than in phosphides or arsenides.

One may wonder if it is possible to predict which alloy system will exhibit localization. Qualitatively, one expects localization of electron states in an  $A_{1-x}B_x$  alloy if the conduction-band minimum of the dilute “impurity” species lies significantly below that of the host majority species, and the impurity electron mass is sufficiently heavy. Under these conditions we expect electron confinement, although atomic relaxation may change the overall picture. Accordingly, using the band offset calculations of Wei and Zunger,<sup>77</sup> the CBM of GaN lies below that of GaP (by 0.6 eV) and GaAs (by 0.3 eV), but above those of InN, InP, and InAs (by 1.3, 0.2, and 0.8 eV, respectively), so only in the former group one expects electron localization for nitrogen-dilute alloys, especially considering the rather heavy electron mass of GaN ( $\sim 0.13m_e$ ). Localization is also expected for dilute InN in

GaP, GaAs, InP, and InAs. Conversely, since the electron mass of InAs is exceedingly light ( $0.02m_e$ ), only a very large host material conduction-band barrier could lead to localization in InAs-dilute alloys. Thus alloys with InAs tend to have only extended states.

### VIII. CONCLUSIONS

The multiband empirical pseudopotential method and atomistically relaxed large supercells are used to study the evolution of the electronic structure of  $\text{GaP}_{1-x}\text{N}_x$  and  $\text{GaAs}_{1-x}\text{N}_x$  alloys, from the isolated nitrogen impurity in the dilute limit, through the formation of nitrogen pairs and clusters, to the formation of the nitride alloy. Our results support a unified theory of alloy formation involving the interactions between nitrogen-induced localized cluster states and the many perturbed host states of the underlying host GaP or GaAs crystal.

We show that isolated nitrogen impurities introduce a highly localized state near the conduction-band minimum. The position of this state is mediated by the GaP/GaN and GaAs/GaN valence-band offset and relaxation of the host lattice near the impurity site. At dilute concentrations ( $\sim 0.01\%$ ) we find this level  $\sim 30$  meV inside the band gap in GaP and resonant  $\sim 180$  meV within the conduction band in GaAs, in quantitative agreement with experiment. Although the isolated nitrogen impurity state is highly localized, we show that it interacts strongly with other nitrogen impurities due to long-ranged lattice relaxation and the long tails evident in the calculated wave functions. Due to this strong interaction we show that it is essential to model the (naturally occurring) heterogeneous distribution of nitrogen atoms (pairs, clusters, etc.), that has been neglected in earlier alloy models.

For the *isolated impurity* we find that the following. (i) Contrary to previous expectations, lattice relaxation *deepens* the nitrogen impurity level due to the increased nitrogen-induced relaxation, which increases the interband couplings. In GaP:N, relaxation introduces some  $\Gamma$  character to the lowest gap level, thus changing it from dipole-forbidden to dipole-allowed (“direct gap”). (ii) *Isolated* nitrogen impurities (rather than a random distribution of *interacting* nitrogen impurities) already create large bowing of the band gap; thus large bowing is an intrinsic effect unrelated to impurity clustering. (iii) The interaction of the nitrogen impurity state,  $a_1(\text{N})$ , with other symmetry-compatible host-perturbed states leads to an anticrossing behavior with applied pres-

sure. In GaP:N, these interactions result in a low pressure coefficient for the impurity state, while in GaAs:N the isolated emerges into the band gap at  $\sim 2$  GPa.

For *impurity pairs* we find, in agreement with experiment, that in GaP:N, the interaction of nitrogen pairs forms a complex series of band gap levels up to  $\sim 180$  meV below the conduction-band edge. For GaAs:N only the first- and fourth-neighbor pairs are calculated to create gap levels. We demonstrate the strong influence of lattice relaxation and multi-band coupling on the energies and character of the nitrogen pair states and show, contrary to historic assumptions, that the energy levels associated with  $m$ th nearest neighbor N-N pairs are a *nonmonotonic* function of the pair separation. We also find that the NN2 line observed in photoluminescence is due to a nitrogen *triplet* and not, often assumed, a second-nearest-neighbor *pair*. For prototypical *nitrogen clusters* we find that multiple nitrogen atoms centered around a single gallium atom result in progressively deeper gap levels, and demonstrate that while any nitrogen impurities will create gap levels in GaP, a local nitrogen concentration of 2–3 atoms is required in GaAs.

With *increasing nitrogen concentration*, we find that (i) the localized cluster states due to pairs, triplets, and clusters do not immediately form an impurity band, and instead the delocalized perturbed host states move into the fundamental band gap and gradually overtake the cluster states. (ii) The conduction-band edge exhibits alloy fluctuations due to localized cluster states and delocalized perturbed host states at the same energy. The low-energy side of the band edge is dominated by cluster states while the higher end consists also of more extended host states. (iii) The localized-delocalized nature of the conduction-band edge leads to localization in tail states, a Stokes shift between emission and absorption, and anomalous temperature and pressure effects.

Our theory of  $\text{GaAs}_{1-x}\text{N}_x$  and  $\text{GaP}_{1-x}\text{N}_x$  alloy formation, from the dilute nitrogen regime (0.01%) through to alloys ( $\geq 3\%$ ), is fully supported by recent emission and absorption measurements (e.g., Refs. 23,37,28,32,33,39,45–48,40,51 and 54), BEEM,<sup>56</sup> and Raman measurements,<sup>52</sup> and explains many of the electronic anomalies and puzzling phenomenology of these materials.

### ACKNOWLEDGMENTS

This work was supported by the U.S. Department of Energy, SC-BES-OER Grant No. DE-AC36-98-GO10337. We are grateful to B. Gil and M. Capizzi for helpful discussions.

<sup>1</sup>D. G. Thomas, J. J. Hopfield, and C. J. Frosch, Phys. Rev. Lett. **15**, 857 (1965).

<sup>2</sup>D. G. Thomas and J. J. Hopfield, Phys. Rev. **150**, 680 (1966).

<sup>3</sup>M. Kondow *et al.*, Jpn. J. Appl. Phys., Part 1 **35**, 1273 (1996).

<sup>4</sup>J. Geisz *et al.*, J. Cryst. Growth **195**, 401 (1998).

<sup>5</sup>E. Cohen *et al.*, Phys. Rev. Lett. **35**, 1591 (1975).

<sup>6</sup>E. Cohen and M. D. Sturge, Phys. Rev. B **15**, 1039 (1977).

<sup>7</sup>D. J. Wolford, J. A. Bradley, K. Fry, and J. Thompson, in *Pro-*

*ceedings of the 17th International Conference of the Physics of Semiconductors* (Springer, New York, 1984), p. 627.

<sup>8</sup>J. D. Perkins *et al.*, Phys. Rev. Lett. **82**, 3312 (1999).

<sup>9</sup>X. Liu *et al.*, Appl. Phys. Lett. **56**, 1451 (1990).

<sup>10</sup>X. Liu, M.-E. Pistol, and L. Samuelson, Phys. Rev. B **42**, 7504 (1990).

<sup>11</sup>P. Vogl, Festkoerperprobleme **XXI**, 191 (1981).

<sup>12</sup>M. I. Eremets, O. A. Krasnovskij, V. V. Struzhkin, and A. M.

- Shirokov, *Semicond. Sci. Technol.* **4**, 267 (1989).
- <sup>13</sup>B. Gil *et al.*, *Phys. Rev. B* **29**, 3398 (1984).
- <sup>14</sup>*Numerical Data and Functional Relationships in Science and Technology*, edited by Landolt-Börnstein (Springer-Verlag, Berlin, 1987), Vol. 22a.
- <sup>15</sup>A. Zunger, in *Solid State Physics*, edited by H. Ehrenreich, D. Turnbull, and Seitz (Academic, Boston, 1986), Vol. 39, p. 275.
- <sup>16</sup>R. Magri, S. Froyen, and A. Zunger, *Phys. Rev. B* **44**, 7947 (1991).
- <sup>17</sup>A. Zunger and J. Jaffe, *Phys. Rev. Lett.* **51**, 662 (1983).
- <sup>18</sup>J. Bernard and A. Zunger, *Phys. Rev. B* **36**, 3199 (1987).
- <sup>19</sup>S.-H. Wei and A. Zunger, *Phys. Rev. B* **43**, 1662 (1991).
- <sup>20</sup>K. Mader and A. Zunger, *Phys. Rev. B* **51**, 10 462 (1995).
- <sup>21</sup>H. Yaguchi *et al.*, *J. Cryst. Growth* **170**, 353 (1997).
- <sup>22</sup>X. Liu, S. G. Bishop, J. N. Baillargeon, and K. Y. Cheng, *Appl. Phys. Lett.* **63**, 1993 (1993).
- <sup>23</sup>H. P. Xin and C. W. Tu, *Appl. Phys. Lett.* **76**, 1267 (2000).
- <sup>24</sup>R. Schwabe *et al.*, *Solid State Commun.* **55**, 167 (1985).
- <sup>25</sup>T. Makimoto, H. Saito, T. Nishida, and N. Kobayashi, *Appl. Phys. Lett.* **70**, 2984 (1997).
- <sup>26</sup>T. Makimoto, H. Saito, and N. Kobayashi, *Jpn. J. Appl. Phys., Part 1* **36**, 1694 (1997).
- <sup>27</sup>H. Saito, T. Makimoto, and N. Kobayashi, *J. Cryst. Growth* **170**, 372 (1997).
- <sup>28</sup>P. J. Klar *et al.*, *Appl. Phys. Lett.* **76**, 3439 (2000).
- <sup>29</sup>P. Leroux-Hugon and H. Mariette, *Phys. Rev. B* **30**, 1622 (1984).
- <sup>30</sup>H. Mariette, *Physica B* **146B**, 286 (1987).
- <sup>31</sup>H. Grüning *et al.*, *Phys. Status Solidi B* **215**, 39 (1999).
- <sup>32</sup>I. A. Buyanova *et al.*, *Appl. Phys. Lett.* **77**, 2325 (2000).
- <sup>33</sup>Y. Zhang *et al.*, *Phys. Rev. B* **62**, 4493 (2000).
- <sup>34</sup>M. J. Caldas, A. Fazzio, and A. Zunger, *Appl. Phys. Lett.* **45**, 671 (1984).
- <sup>35</sup>N. Mott, *Metal-Insulator Transition* (Taylor and Francis, London, 1974).
- <sup>36</sup>I. A. Buyanova *et al.*, *Appl. Phys. Lett.* **75**, 3781 (1999).
- <sup>37</sup>H. P. Xin and C. W. Tu, *Appl. Phys. Lett.* **77**, 2180 (2000).
- <sup>38</sup>H. Yaguchi *et al.*, *Solid-State Electron.* **41**, 231 (1997).
- <sup>39</sup>Y. Zhang *et al.*, *Phys. Rev. B* **63**, 085205 (2001).
- <sup>40</sup>I. A. Buyanova *et al.*, *Phys. Status Solidi B* **216**, 125 (1999).
- <sup>41</sup>J. Toivonen, T. Hakkarainen, M. Sopenan, and H. Lipsanen, *J. Cryst. Growth* **221**, 456 (2000).
- <sup>42</sup>Y. Zhang, A. Mascarenhas, H. P. Xin, and C. W. Tu, *Phys. Rev. B* **61**, 7479 (2000).
- <sup>43</sup>P. N. Hai *et al.*, *Appl. Phys. Lett.* **77**, 1843 (2000).
- <sup>44</sup>K. M. Yu *et al.*, *Phys. Rev. B* **61**, R13 337 (2000).
- <sup>45</sup>K. Uesugi *et al.*, *Appl. Phys. Lett.* **76**, 1285 (2000).
- <sup>46</sup>A. Polimeni *et al.*, *Appl. Phys. Lett.* **77**, 2870 (2000).
- <sup>47</sup>H. Yaguchi *et al.*, *J. Cryst. Growth* **189/190**, 496 (1998).
- <sup>48</sup>K. Onabe, D. Aoki, J. Wu, and Y. Yaguchi, and H. Shiraki, *Phys. Status Solidi A* **176**, 231 (1999).
- <sup>49</sup>T. Mattila, S.-H. Wei, and A. Zunger, *Phys. Rev. Lett.* **83**, 2010 (1999).
- <sup>50</sup>M. Takahashi *et al.*, *J. Cryst. Growth* **221**, 461 (2000).
- <sup>51</sup>W. Shan *et al.*, *Phys. Rev. Lett.* **82**, 1221 (1999).
- <sup>52</sup>H. M. Cheong, Y. Zhang, A. Mascarenhas, and J. F. Geisz, *Phys. Rev. B* **61**, 13 687 (2000).
- <sup>53</sup>G. Leibiger *et al.*, *Appl. Phys. Lett.* **77**, 1650 (2000).
- <sup>54</sup>W. Shan *et al.*, *Appl. Phys. Lett.* **76**, 3251 (2000).
- <sup>55</sup>W. Shan *et al.*, *Phys. Rev. B* **62**, 4211 (2000).
- <sup>56</sup>M. Kozhevnikov *et al.*, *Phys. Rev. B* **61**, R7861 (2000).
- <sup>57</sup>W. G. Bi and C. W. Tu, *Appl. Phys. Lett.* **69**, 3710 (1996).
- <sup>58</sup>L. Bellaïche, S.-H. Wei, and A. Zunger, *Phys. Rev. B* **56**, 10 233 (1997).
- <sup>59</sup>J. N. Baillargeon *et al.*, *Appl. Phys. Lett.* **60**, 2540 (1992).
- <sup>60</sup>A. Lindsay and E. P. O'Reilly, *Solid State Commun.* **112**, 443 (1999).
- <sup>61</sup>A. Zunger, S.-H. Wei, L. Ferreira, and J. Bernard, *Phys. Rev. Lett.* **65**, 353 (1990).
- <sup>62</sup>T. Mattila, S.-H. Wei, and A. Zunger, *Phys. Rev. B* **60**, R11 245 (1999).
- <sup>63</sup>L. Bellaïche, S.-H. Wei, and A. Zunger, *Phys. Rev. B* **54**, 17 568 (1996).
- <sup>64</sup>L. Bellaïche, S.-H. Wei, and A. Zunger, *Appl. Phys. Lett.* **70**, 3558 (1997).
- <sup>65</sup>L. Bellaïche and A. Zunger, *Phys. Rev. B* **57**, 4425 (1998).
- <sup>66</sup>T. Mattila, L.-W. Wang, and A. Zunger, *Phys. Rev. B* **59**, 15 270 (1999).
- <sup>67</sup>E. D. Jones *et al.*, *Phys. Rev. B* **60**, 4430 (1999).
- <sup>68</sup>R. M. Martin, *Phys. Rev. B* **1**, 4005 (1970).
- <sup>69</sup>L. Wang and A. Zunger, *J. Chem. Phys.* **100**, 2394 (1994).
- <sup>70</sup>L.-W. Wang, L. Bellaïche, S.-H. Wei, and A. Zunger, *Phys. Rev. Lett.* **80**, 4725 (1998).
- <sup>71</sup>M. Jaros and S. Brand, *J. Phys. C* **12**, 525 (1979).
- <sup>72</sup>M. Jaros, *Deep Levels in Semiconductors* (Adam Hilger, Bristol, 1982).
- <sup>73</sup>G. F. Bassani and G. Pastori Parravicini, in *Electronic States and Optical Transitions in Solids*, edited by R. A. Ballinger (Pergamon, New York, 1975).
- <sup>74</sup>J. Leymarie, M. Leroux, and G. Neu, *Phys. Rev. B* **42**, 1482 (1990).
- <sup>75</sup>T. N. Morgan, *Phys. Rev. Lett.* **21**, 819 (1968).
- <sup>76</sup>T. G. Caster, *Phys. Rev. B* **2**, 4911 (1970).
- <sup>77</sup>S.-H. Wei and A. Zunger, *Appl. Phys. Lett.* **72**, 2011 (1998).
- <sup>78</sup>L.-W. Wang, *Appl. Phys. Lett.* **78**, 1565 (2001).
- <sup>79</sup>Y. Zhang and A. Mascarenhas, *Phys. Rev. B* **61**, 15 562 (2000).
- <sup>80</sup>W. Orellana and A. C. Ferraz, *Appl. Phys. Lett.* **78**, 1231 (2001).
- <sup>81</sup>S. Francoeur *et al.*, *Appl. Phys. Lett.* **75**, 1538 (1999).
- <sup>82</sup>S.-H. Wei and A. Zunger, *Phys. Rev. B* **60**, 5404 (1999).
- <sup>83</sup>A. Baldereschi, *J. Lumin.* **7**, 79 (1973).
- <sup>84</sup>R. G. Dandrea and A. Zunger, *Appl. Phys. Lett.* **57**, 1031 (1990).
- <sup>85</sup>A. Zunger, *Phys. Rev. Lett.* **54**, 849 (1985).
- <sup>86</sup>T. Mattila and A. Zunger, *Phys. Rev. B* **59**, 9943 (1999).
- <sup>87</sup>R. A. Faulkner, *Phys. Rev.* **175**, 991 (1968).
- <sup>88</sup>H. P. Hjalmarson, P. Vogl, D. J. Wolford, and J. D. Dow, *Phys. Rev. Lett.* **44**, 810 (1980).
- <sup>89</sup>M. Kondow, K. Uomi, K. Hosomi, and T. Mozume, *Jpn. J. Appl. Phys., Part 2* **33**, L1056 (1994).
- <sup>90</sup>Y. Zhang, A. Mascarenhas, H. P. Xin, and C. W. Tu, *Phys. Rev. B* **63**, 161303 (2001).
- <sup>91</sup>J. C. Phillips, *Phys. Rev. Lett.* **22**, 285 (1969).
- <sup>92</sup>J. J. Hopfield, D. G. Thomas, and R. T. Lynch, *Phys. Rev. Lett.* **17**, 312 (1996).
- <sup>93</sup>B. Gil, J. Camassel, J. P. Albert, and H. Mathieu, *Phys. Rev. B* **33**, 2690 (1986).
- <sup>94</sup>T. Mattila and A. Zunger, *Phys. Rev. B* **58**, 1367 (1998).
- <sup>95</sup>H. A. McKay, R. M. Feenstra, T. Schmidling, and U. W. Pohl, *Appl. Phys. Lett.* **78**, 82 (2001).
- <sup>96</sup>S. B. Zhang and A. Zunger, *Appl. Phys. Lett.* **71**, 677 (1997).

- <sup>97</sup>S. B. Zhang and S.-H. Wei, Phys. Rev. Lett. **86**, 1789 (2001).
- <sup>98</sup>C. Benoit á la Guillaume, Physica B **117/118B**, 105 (1983).
- <sup>99</sup>J. Shen, S. Y. Ren, and J. D. Dow, Phys. Rev. B **42**, 9119 (1990).
- <sup>100</sup>Y. Zhang and W. Ge, J. Lumin. **85**, 247 (2000).
- <sup>101</sup>B. Gil and H. Mariette, Phys. Rev. B **35**, 7999 (1987).
- <sup>102</sup>H. P. Xin, K. L. Kavanagh, Z. Q. Zhu, and C. W. Tu, Appl. Phys. Lett. **74**, 2337 (1999).
- <sup>103</sup>R. K. Ahrenkiel, S. W. Johnston, B. M. Keyes, and D. J. Friedman, Appl. Phys. Lett. **77**, 3794 (2000).
- <sup>104</sup>Y. Zhang, A. Mascarenhas, H. P. Xin, and C. W. Tu, Phys. Rev. B **61**, 4433 (2000).
- <sup>105</sup>S. Sakai, Y. Ueta, and Y. Terauchi, Jpn. J. Appl. Phys., Part 1 **32**, 4413 (1993).
- <sup>106</sup>L. Bellaiche, Appl. Phys. Lett. **75**, 2578 (1999).
- <sup>107</sup>K. Uesugi, N. Morooka, and I. Suemune, Appl. Phys. Lett. **74**, 1254 (1999).